

NASA Contractor Report 3466

NASA
CR
3466
c.1



Development of the Triplet Singularity for the Analysis of Wings and Bodies in Supersonic Flow

F. A. Woodward

LOAN COPY: RETURN TO
AFWL TECHNICAL LIBRARY
KIRTLAND AFB, N.M.

CONTRACT NAS1-15792
SEPTEMBER 1981





NASA Contractor Report 3466

Development of the Triplet Singularity for the Analysis of Wings and Bodies in Supersonic Flow

F. A. Woodward
Analytical Methods, Inc.
Bellevue, Washington

Prepared for
Langley Research Center
under Contract NAS1-15792

NASA

National Aeronautics
and Space Administration

**Scientific and Technical
Information Branch**

1981

TABLE OF CONTENTS

SUMMARY	1
INTRODUCTION	1
LIST OF SYMBOLS	2
AERODYNAMIC THEORY	4
Body Triplet Singularities	4
Wing Triplet Singularities	16
APPLICATION	18
Body Panel Arrangement	18
Wing Panel Arrangement	18
EXAMPLES	22
Parabolic Body of Revolution	22
Cone-Cylinder-Cone	22
Nacelle with Internal Flow	22
Ogive-Cylinder-Boattail	29
Elliptic Cone	29
B-1 Forebody	29
Uncambered Arrow Wing	29
Cambered Arrow Wing	37
CONCLUSIONS	41
APPENDIX A: DERIVATION OF BODY SINGULARITIES	42
APPENDIX B: DERIVATION OF WING SINGULARITIES	57
REFERENCES	69

SUMMARY

A supersonic triplet singularity has been developed which eliminates internal waves generated by panels having supersonic edges. The triplet is a linear combination of source and vortex distributions which gives directional properties to the perturbation flow field surrounding the panel. The theoretical development of the triplet singularity is described together with its application to the calculation of surface pressures on wings and bodies. Examples are presented comparing the results of the new method with other supersonic methods and with experimental data.

INTRODUCTION

Significant advances have been made in the application of surface singularity techniques to the analysis and design of complex aircraft configurations in both subsonic and supersonic flows, (Refs. 1 and 2). The success of these methods is primarily due to the use of high-order source, vortex, or doublet singularities on surface panels, and by improvements in the formulation of the boundary conditions.

The use of surface panel singularities in supersonic flow introduces jumps in the perturbation velocity flow field across the Mach waves originating along the panel leading and trailing edges. If these waves propagate into the interior of the wing or body, they can induce spurious perturbations on the opposite side of the configuration and seriously affect the strength of the surface singularity distribution.

The supersonic triplet singularity is designed to eliminate the spurious internal waves generated by panels having supersonic leading edges. In particular, the perturbation velocities in the "two-dimensional" region associated with supersonic panel edges are exactly cancelled in the interior flow. This results in a well conditioned system of boundary condition equations and a corresponding improvement in the pressure distribution calculated on the exterior of the configuration.

The application of the supersonic triplet concept to the aerodynamic analysis of bodies having arbitrary cross-section is reported in Ref. 3. This report describes the extension of the method to the analysis of swept, tapered wings, and includes details on the derivation of the wing and body triplet singularities. In addition, examples are presented comparing the results of this method with other supersonic methods and experimental data.

LIST OF SYMBOLS

a	Panel inclination = $\tan \delta$ Panel taper ratio
b	Panel span
c	Panel chord
C	Constant
d	Hyperbolic distance to panel corner
D	Hyperbolic distance to panel apex
F,G,H	Velocity distribution functions
ℓ	Distance from panel apex to origin
m	Panel edge slope = $\tan \delta$
M	Mach number
r, θ	Angular coordinates
u, v, w	Perturbation velocities
x, y, z	Cartesian coordinates
α	Angle of attack
β	Prandtl-Glauert factor = $\sqrt{M^2 - 1}$
γ	Geometric parameter
δ	Panel inclination angle
λ	Leading-edge sweep = $\tan \Lambda$
Λ	Leading-edge sweep angle
τ	$\sqrt{\beta^2 - \lambda^2}$
ξ, η	Integration variables

Subscripts

A	Axial
C	Circumferential, constant
E	Edge
L	Line
R	Radial
S	Source
T	Triplet
V	Vortex

AERODYNAMIC THEORY

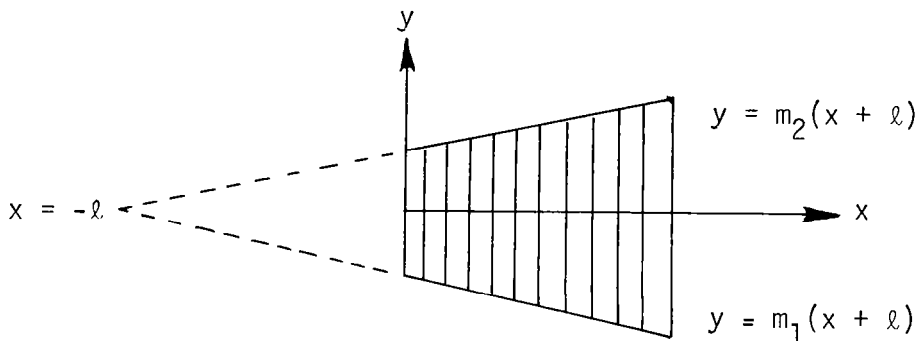
The triplet singularity is a linear combination of source and vortex singularity distributions. Since the vortex (or doublet) sheet may be considered the result of combining, in a special limiting process, two source sheets of equal and opposite strength, the combination of a vortex sheet of unit strength with a source sheet of strength $\tau = \sqrt{\beta^2 - \lambda^2}$, has been termed a triplet. The procedure is only applicable to panels having supersonic leading edges, corresponding to real values for τ . A simple illustration of the basic concept for two-dimensional flow is given in Figure 1. In this example, the axial and normal velocity component vectors add in the flow field above the panel, but cancel exactly below the panel, resulting in the desired unidirectional perturbation velocity field.

The extension of this concept to the analysis of three-dimensional bodies and wings is described in the following sections.

Body Triplet Singularities

Three types of triplet singularities are required to apply this method to bodies having arbitrary cross-section. They are designated circumferential, edge, or radial, depending on the orientation of the elementary line singularities used in the derivation. An axial triplet singularity can also be obtained by combining the circumferential and edge triplets.

Circumferential Triplet. The circumferential triplet is obtained by combining a circumferential source and vortex distribution. The elementary source and vortex filaments making up these singularities lie in the plane of the panel, parallel to the y-axis, as indicated on the following sketch. Note that the side edges of the panel intersect the x-axis a distance, ℓ , ahead of the origin.



TWO-DIMENSIONAL FLOW

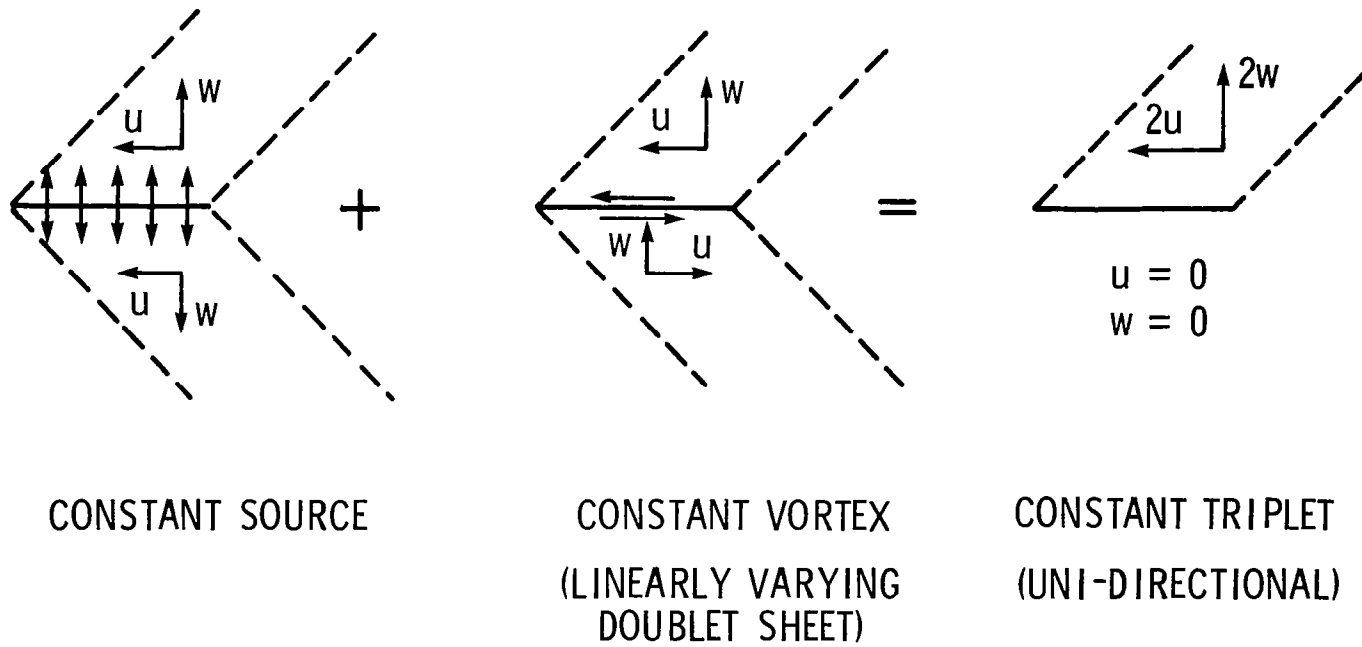


Figure 1. - Supersonic Triplet Concept.

The three components of velocity induced at a point, x, y, z , in the field by one corner of the panel are derived in Appendix A. The influence of the vortex distribution is given by Eqns. (A12) through (A14), and the source distribution by Eqns. (A15) through (A17). The circumferential triplet is obtained by combining these singularities as follows.

$$\begin{aligned} u'_{TC} &= u_{VC} + \beta u_{SC} \\ &= F + H - \beta m G \end{aligned} \quad (1)$$

$$\begin{aligned} v'_{TC} &= v_{VC} + \beta v_{SC} \\ &= \beta G \end{aligned} \quad (2)$$

$$\begin{aligned} w'_{TC} &= w_{VC} + \beta w_{SC} \\ &= \beta(\beta m G - F - H) \\ &= -\beta u'_{TC} \end{aligned} \quad (3)$$

where

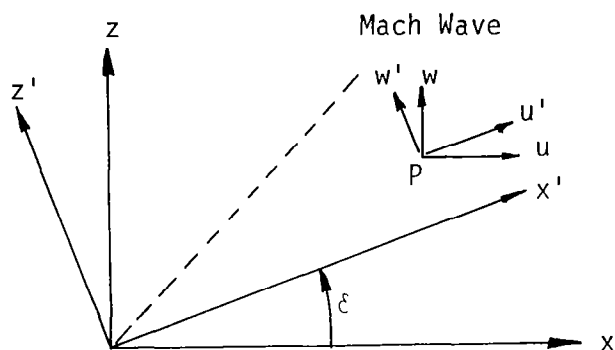
$$F = \tan^{-1} \frac{z \sqrt{x^2 - \beta^2(y - m\ell)^2 - \beta^2 z^2}}{x(m(x + \ell) - y) - \beta^2 m z^2} \quad (4)$$

$$G = \frac{1}{\sqrt{1 - \beta^2 m^2}} \cosh^{-1} \frac{x - \beta^2 m(y - m\ell)}{\beta \sqrt{(y - m(x + \ell))^2 + (1 - \beta^2 m^2) z^2}} \quad (5)$$

$$H = \sin^{-1} \frac{\beta(y - m\ell)}{\sqrt{x^2 - \beta^2 z^2}} \quad (6)$$

Within the two-dimensional flow region (ahead of the Mach cones from the inboard and outboard corners of the panel, and behind the Mach wave from the unswept leading edge), $F = \pi$ above the plane of the panel, and $-\pi$ below, while $H = \pi$ within this region on both sides of the panel. Thus the sum $F + H$ appearing in Eqn. (1) and (3) has a value of 2π above the panel, and zero below. This special relationship provides the desired wave cancellation property of the triplet singularity.

The three components of velocity induced by a panel inclined at an angle, δ , to the x-y plane are obtained by applying a Lorentz transformation about the y-axis. The geometry is illustrated on the following sketch.



For a panel lying in the x',y' plane, and defining $a = \tan \delta$,

$$u = \frac{u' - aw'}{\sqrt{1 - \beta^2 a^2}} \quad (7)$$

$$v = v' \quad (8)$$

$$w = \frac{w' - \beta^2 au'}{\sqrt{1 - \beta^2 a^2}} \quad (9)$$

Expressions for the velocity components in the primed system of coordinates are given by Eqns. (1) through (3). Substituting

$$x' = \frac{x - \beta^2 az}{\sqrt{1 - \beta^2 a^2}} \quad (10)$$

$$y' = y \quad (11)$$

$$z' = \frac{z - ax}{\sqrt{1 - \beta^2 a^2}} \quad (12)$$

$$m' = \frac{m}{\sqrt{1 - \beta^2 a^2}} \quad (13)$$

The transformed velocity components in the reference coordinate system become:

$$u_{TC} = \frac{F + H - \beta m G}{1 - \beta a} \quad (14)$$

$$v_{TC} = G \quad (15)$$

$$w_{TC} = -\beta u_{TC} \quad (16)$$

with

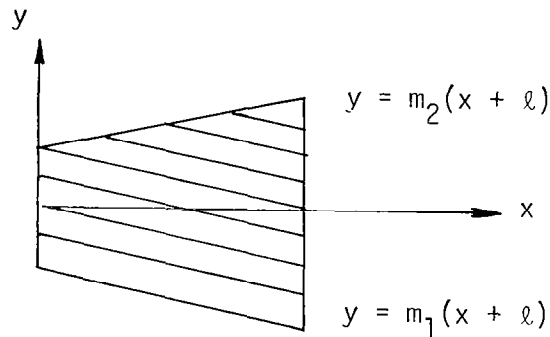
$$F = \tan^{-1} \frac{(z - ax) \sqrt{x^2 - \beta^2 (y - ml)^2 - \beta^2 z^2}}{x[m(x + l) + y] + \beta^2 z [ay - m(z + al)]} \quad (17)$$

$$G = \frac{1}{\sqrt{1 - \beta^2(a^2 + m^2)}}$$

$$\cosh^{-1} \frac{x - \beta^2[m(y - m\ell) + az]}{\beta\sqrt{[y - m(x + \ell)]^2 - \beta^2[ay - m(z + a\ell)]^2 + (z - ax)^2}} \quad (18)$$

and H is given by Eqn. (6).

Edge Triplet. The edge triplet is obtained by combining edge source and vortex distributions. The elementary source and vortex filaments making up these singularities lie in the plane of the panel parallel to one edge, as indicated on the following sketch.



The three components of velocity induced at a point, x, y, z , in the field by one corner of the panel are derived in Appendix A. The influence of the vortex distribution is given by Eqns. (A24) - (A26), and the source distribution by (A27) - (A29). In addition, the influence of a linearly varying line vortex along the leading edge (Eqns. (A57) - (A59)) is added to the vortex distribution, and a linearly varying line source along the leading edge (Eqns. (A63) - (A65)) is added to the source distribution. Combining these four contributions, the three components of velocity for the edge triplet singularity may be written:

$$\begin{aligned}
u'_{TE} &= u_{VE} + u_{VL} + \beta(u_{SE} + u_{SL}) \\
&= \frac{1}{\beta} \left[\frac{D}{x - \beta z} - \beta m(F + H - \beta mG) \right]
\end{aligned} \tag{19}$$

$$\begin{aligned}
v'_{TE} &= v_{VE} + v_{VL} + \beta(v_{SE} + v_{SL}) \\
&= F + H - \beta mG
\end{aligned} \tag{20}$$

$$\begin{aligned}
w'_{TE} &= w_{VE} + w_{VL} + \beta(w_{SE} + w_{SL}) \\
&= G + \beta m(F + H - \beta mG) - \frac{D}{x - \beta z} \\
&= G - \beta u'_{TE}
\end{aligned} \tag{21}$$

where F, G, and H are given by Eqns. (4) - (6), and

$$D = \sqrt{x^2 - \beta^2(y - ml)^2 - \beta^2 z^2} \tag{22}$$

Applying a Lorentz transformation by substituting Eqns. (19) - (21) in Eqns. (7) - (9), the three components of velocity induced at a point, x,y,z, in the reference coordinate system by an inclined panel can be written:

$$u_{TE} = \frac{1}{\beta} \left[\frac{D}{x - \beta z} - \frac{\beta m}{1 - \beta a} v_{TE} - \beta a G \right] \tag{23}$$

$$v_{TE} = F + H - \beta m G \quad (24)$$

$$w_{TE} = G - \beta u_{TE} \quad (25)$$

where F and G are given by Eqns. (17) and (18), H by Eqn. (6), and D by Eqn. (22).

Axial Triplet. The influence of an axial triplet distribution on an inclined panel can be obtained by adding the influence of an edge triplet to the influence of a circumferential triplet multiplied by the factor, βm . Combining Eqns. (23) - (25) with Eqns. (14) - (16), the three components of velocity can be written:

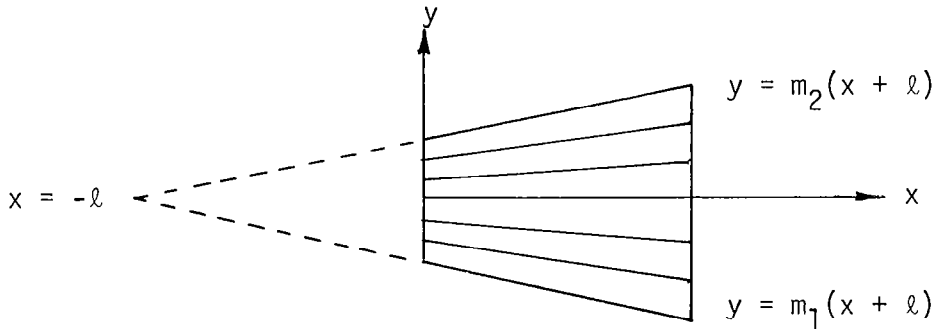
$$\begin{aligned} u_{TA} &= u_{TE} + \beta m u_{TC} \\ &= \frac{1}{\beta} \left[\frac{D}{x - \beta z} - \beta a G \right] \end{aligned} \quad (26)$$

$$\begin{aligned} v_{TA} &= v_{TE} + \beta m v_{TC} \\ &= F + H \end{aligned} \quad (27)$$

$$\begin{aligned} w_{TA} &= w_{TE} + \beta m w_{TC} \\ &= G - \frac{D}{x - \beta z} \end{aligned} \quad (28)$$

This corresponds to a triplet distribution having the elementary source and vortex filaments parallel to the x-axis.

Radial Triplet. The elementary source and vortex filaments making up the radial triplet distribution lie in the plane of the panel along radial lines from the intersection of the two side edges extended. This point lies on the x-axis a distance, ℓ , ahead of the origin, as indicated on the following sketch.



The three components of velocity induced at a point, x, y, z , by one corner of the panel are derived in Appendix A. The influence of the vortex distribution is given by Eqns. (A39) - (A41), and the source distribution by Eqns. (A57) - (A59).

In addition, the influence of a linearly varying line vortex along the leading edge (Eqns. (A57) - (A59)) is added to the vortex distribution, and a linearly varying line source along the leading edge (Eqns. (A63) - (A65)) is added to the source distribution. Combining these four contributions, the three components of velocity for the radial triplet singularity may be written:

$$\begin{aligned}
 u'_{TR} &= u_{VR} + u_{VL} + \beta(u_{SR} + u_{SL}) \\
 &= \frac{-\ell}{\beta(x + \ell - \beta z)} \left[\frac{\beta y}{x + \ell - \beta z} (F + H - \beta y G_R) - \frac{D}{x - \beta z} + \beta z G_R \right]
 \end{aligned}
 \tag{29}$$

$$\begin{aligned}
v'_{TR} &= v_{VR} + v_{VL} + \beta(v_{SR} + v_{SL}) \\
&= \frac{\ell}{x + \ell - \beta z} (F + H - \beta y G_R)
\end{aligned} \tag{30}$$

$$\begin{aligned}
w'_{TR} &= w_{VR} + w_{VL} + \beta(w_{SR} + w_{SL}) \\
&= \frac{\ell}{x + \ell - \beta z} \left[\frac{\beta y}{x + \ell - \beta z} (F + H - \beta y G_R) - \frac{D}{x - \beta z} + (x + \ell) G_R \right]
\end{aligned} \tag{31}$$

where F is given by Eqn. (4),
 H is given by Eqn. (6),
 D is given by Eqn. (22),

$$G_R = \frac{1}{D_R} \cosh^{-1} \frac{x(x + \ell) - \beta^2 y(y - m\ell) - \beta^2 z^2}{\beta \ell \sqrt{(y - m(x + \ell))^2 + (1 - \beta^2 m^2) z^2}} \tag{32}$$

and $D_R = \sqrt{(x + \ell)^2 - \beta^2 y^2 - \beta^2 z^2}$ \tag{33}

Applying a Lorentz transformation, by substituting Eqns. (29) - (31) in Eqns. (7) - (9), the three components of velocity at a point, x, y, z , in the reference coordinate system by an inclined panel become:

$$u_{TR} = \frac{-c}{\beta} \left\{ \frac{\beta y}{x + \ell - \beta(z + a\ell)} (F + H - \beta y G_R) - \frac{D}{x - \beta z} + \beta(z + a\ell) G_R \right\} \tag{34}$$

$$v_{TR} = c(F + H - \beta y G_R) \quad (35)$$

$$w_{TR} = c \left\{ \frac{\beta y}{x + \ell - \beta(z + a\ell)} (F + H - \beta y G_R) - \frac{D}{x - \beta z} + (x + \ell) G_R \right\} \quad (36)$$

where $c = \frac{(1 - \beta a)\ell}{x + \ell - \beta(z + a\ell)}$

and F is given by Eqn. (17)

H is given by Eqn. (6)

D is given by Eqn. (22)

D_R is given by Eqn. (33)

and $G_R = \frac{1}{D_R} \cosh^{-1} \frac{x(x + \ell) - \beta^2 y(y - m\ell) - \beta^2 z(z + a\ell)}{\beta \ell \sqrt{(y - m(x + \ell))^2 - \beta^2 (ay - m(z + a\ell))^2 + (z - ax)^2}}$ (37)

Rectangular Triplet. For the special case of a rectangular panel, $m = 0$ and $\ell \rightarrow \infty$. Taking this limit,

$$u_{TR} = u_{TE} = u_{TA} = \frac{1}{\beta} \left(\frac{D}{x - \beta z} - \beta a G \right) \quad (38)$$

$$v_{TR} = v_{TE} = v_{TA} = F + H \quad (39)$$

$$w_{TR} = w_{TE} = w_{TA} = G - \frac{D}{x - \beta z} \quad (40)$$

The influence of an edge panel of a triplet panel group is obtained by subtracting the contribution of the radial triplet from that of the edge triplet. This has the effect of distributing the vorticity from a side edge to a trailing edge of a panel. For a rectangular panel, a special limiting process is required to obtain the correct influence.

$$\begin{aligned} u_T &= \lim_{\ell \rightarrow \infty} \left[\ell(u_{TE} - u_{TR}) \right] \\ &= y(F + H) + zG + D/\beta \end{aligned} \quad (41)$$

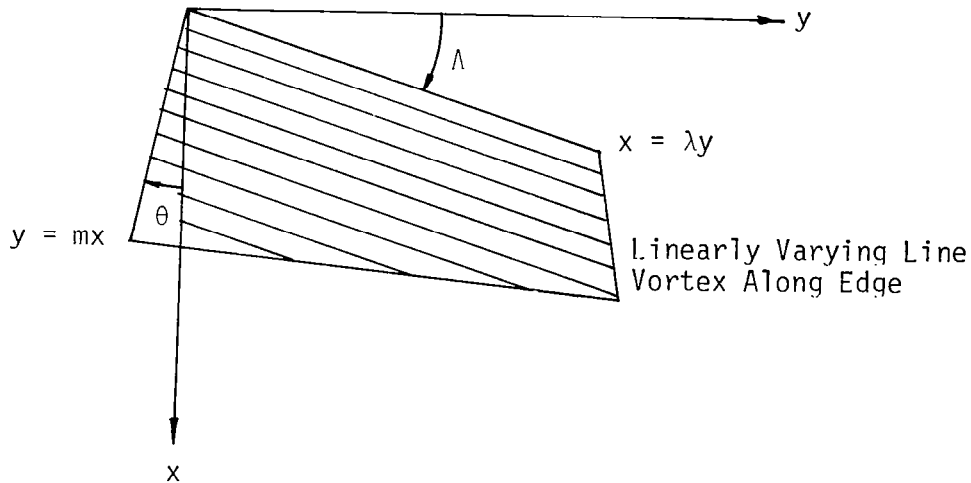
$$\begin{aligned} v_T &= \lim_{\ell \rightarrow \infty} \left[\ell(v_{TE} - v_{TR}) \right] \\ &= (x - \beta z)(F + H) + \beta yG \end{aligned} \quad (42)$$

$$\begin{aligned} w_T &= \lim_{\ell \rightarrow \infty} \left[\ell(w_{TE} - w_{TR}) \right] \\ &= (x - \beta z)G - \beta y(F + H) - 2D \end{aligned} \quad (43)$$

Wing Triplet Singularities

In the analysis of wings, the triplet singularity is required only for those panels having supersonic edges. For panels having sonic or subsonic edges, a combination of constant sources and linearly varying vortices, as described in References 2 and 4, provides a suitable aerodynamic representation. The influence of a constant triplet singularity, located on a panel having a swept supersonic leading edge is derived as follows.

Constant Triplet. The constant triplet is obtained by combining a constant source and vortex distribution. The elementary source and vortex filaments making up these singularities lie in the plane of the panel parallel to the leading edge, as indicated below.



The three components of velocity induced at a point, x, y, z , in the field by one corner of the panel are derived in Appendix B. The influence of a constant vortex distribution is given by Eqns. (B7) - (B9), and a constant source distribution by (B13) - (B15). The constant triplet is obtained by combining these singularities as follows.

$$\begin{aligned}
 u_{TC} &= u_{VC} + \sqrt{\beta^2 - \lambda^2} u_{SC} \\
 &= F + H - m \sqrt{\beta^2 - \lambda^2} G
 \end{aligned}
 \tag{44}$$

$$\begin{aligned}
v_{TC} &= v_{VC} + \sqrt{\beta^2 - \lambda^2} v_{SC} \\
&= -\lambda(F + H) + \sqrt{\beta^2 - \lambda^2} G
\end{aligned} \tag{45}$$

$$\begin{aligned}
w_{TC} &= w_{VC} + \sqrt{\beta^2 - \lambda^2} w_{SC} \\
&= -\sqrt{\beta^2 - \lambda^2} (F + H) - (\lambda - \beta^2 m) G
\end{aligned} \tag{46}$$

where F and G are given by Eqns. (B10) and (B11), and

$$H = \cos^{-1} \frac{\lambda x - \beta^2 y}{\beta \sqrt{(x - \lambda y)^2 + (\lambda^2 - \beta^2 z^2)}} \tag{47}$$

The influence of the complete panel is obtained by combining the influences of each of the four corners. Within the "two-dimensional" region associated with the supersonic leading edge, the sum of F and H is 2π above the plane of the panel, and zero below. This special relationship again provides for cancellation of the perturbation velocities in the interior of the wing.

A pair of linearly varying line vortices is added along the side edges of the panel to transfer the accumulated vorticity into the wake. The influence of these line vortices is given by Eqns. (111) - (113) of Reference 2.

APPLICATION

No special procedures are required to apply the triplet singularities to the analysis of wings and bodies in supersonic flow. One control point is associated with each panel (or group of panels) used in the aerodynamic representation. The boundary condition of tangential flow is then imposed at each control point, and the resulting system of linear equations is solved to determine the individual singularity strengths. Surface pressures, forces, and moments acting on the configuration are then calculated in the usual way. A computer code has been developed to perform the calculations and is available as a modification to the USSAERO program.

Body Panel Arrangement

A panel arrangement suitable for the analysis of a body having arbitrary cross-section is shown in Figure 2. The panel leading and trailing edges are defined by planes perpendicular to the reference x-axis, while panel side edges are defined by the body meridian lines. A grouping of six panels is used to make up a triplet singularity which will satisfy the Helmholtz vortex conservation laws without requiring line vortices along panel edges or trailing vortex wakes. Within this six-panel group, the individual singularity strengths are prescribed to ensure that the elementary vortex filaments form closed loops, as indicated on the figure. The center row of panels contains only circumferential triplet singularities of equal and opposite strengths. The singularities in the outer rows are composed of a special combination of edge and radial triplets, which result in zero vorticity along the outer two edges, and match the inflow (or outflow) of vorticity along the inner two edges.

The strengths of the triplet singularities in each group are determined by satisfying Neumann boundary conditions at the control points.

Wing Panel Arrangement

A conventional panel subdivision is used on the wing. The panel side edges are defined by planes parallel to the reference x-axis, while the leading and trailing edges are defined by constant percent chord lines. Panels are located on both upper and lower surfaces of the wing.

For wings having subsonic leading and trailing edges, a combination of constant sources and linearly varying vortices are used in the aerodynamic representation. The linearly varying vortex singularities are distributed over two adjacent panels, as illustrated in Figure 3, and include a pair of constant vortices trailing downstream along the panel edges and into the wake. The principle of symmetrical singularities is applied, as described in Reference 5, by equating the source and vortex strengths on corresponding

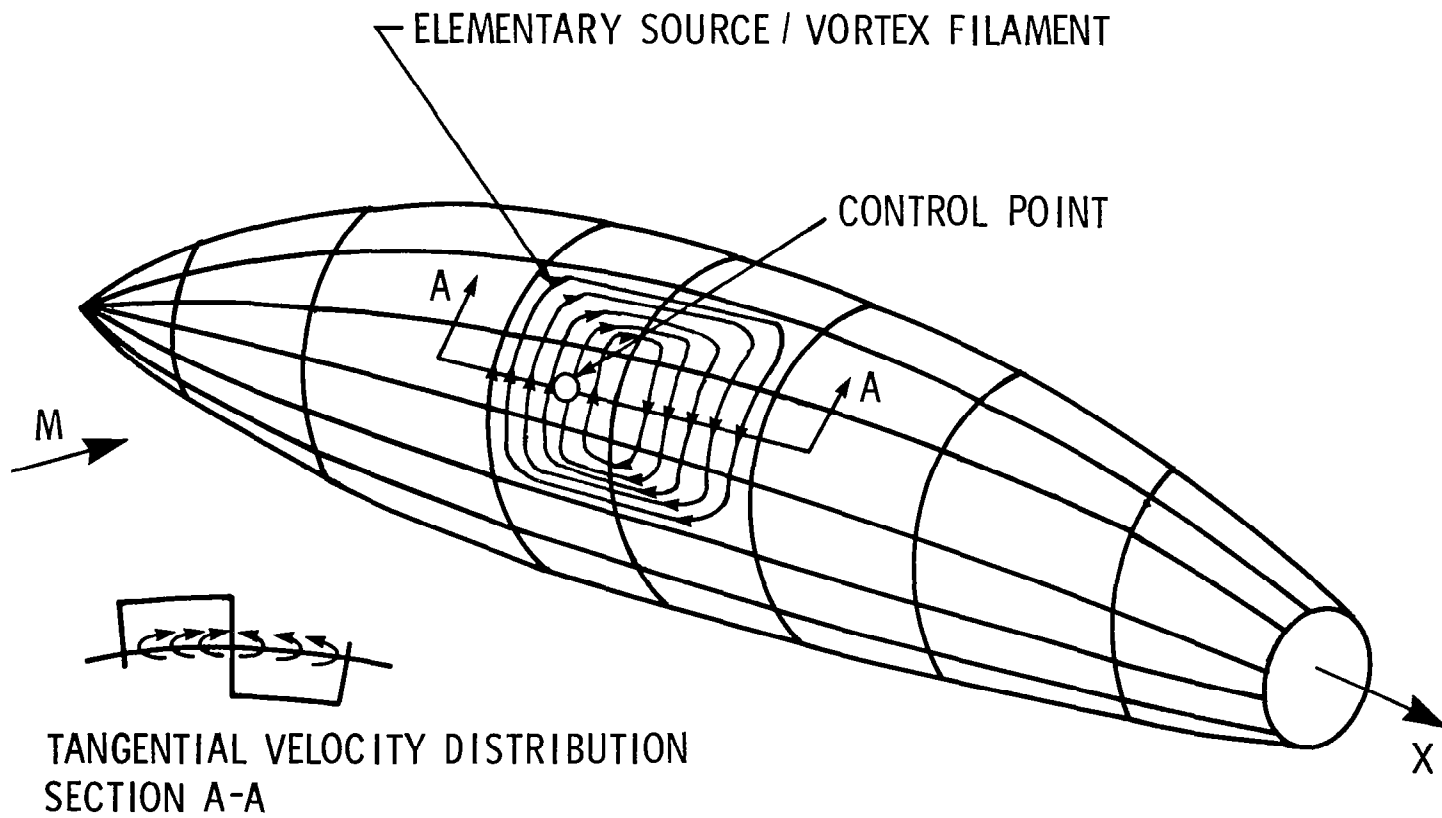


Figure 2. - Panel Arrangement on Arbitrary Body.

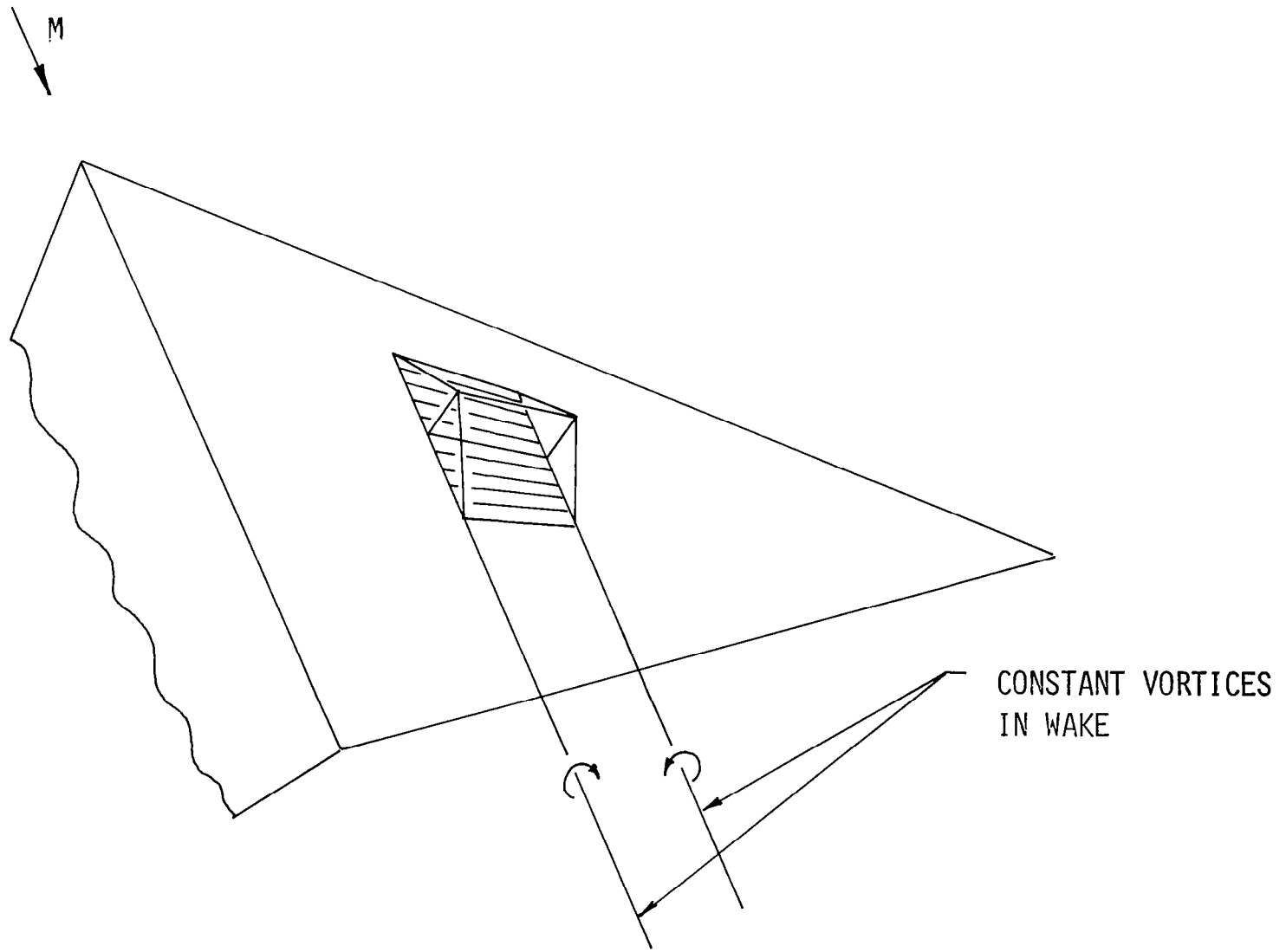
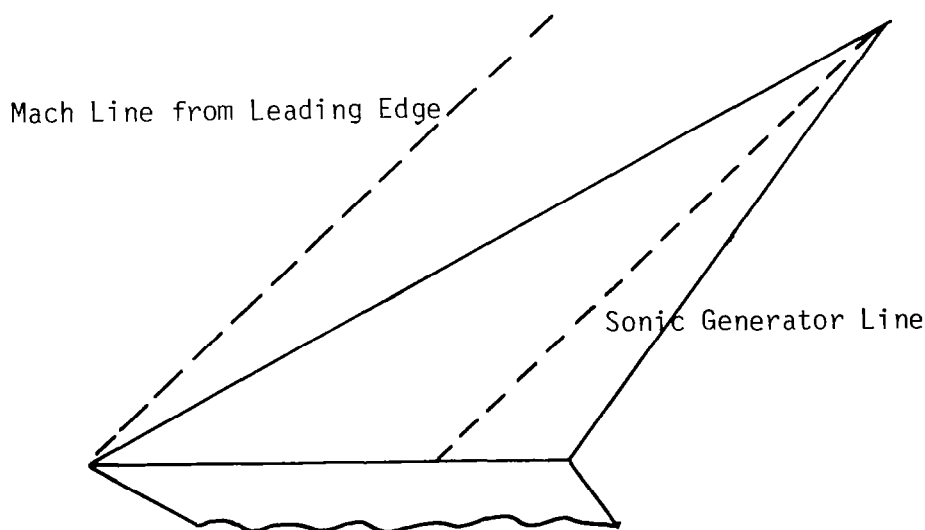


Figure 3. Vortex Panel Arrangement on Wing (Panel has Subsonic Edges).

panels on the upper and lower surfaces of each section. The details of the extension of this method to the analysis of three-dimensional wings is given in Reference 4.

For wings having supersonic leading and trailing edges, constant triplets alone are used on each panel. This aerodynamic representation minimizes interference effects between the upper and lower surfaces of the wing.

Wings having subsonic leading edges and supersonic trailing edges present a more difficult problem. In this case, all panels ahead of the sonic generator line have subsonic edges, and those behind this line have supersonic edges. (A sonic generator line is defined as a wing generator line parallel to the Mach line.) A combination of constant sources and linearly varying vortex singularities are used ahead of this line, changing to constant triplet distributions on panels behind the line, with the linear distributions overlapping the constant distributions on the panel containing the sonic generator line itself. The strengths of the singularities are then determined by applying the symmetrical singularity method described above. This technique results in relatively smooth variations in singularity strength across the sonic generator line.



EXAMPLES

Several examples are presented to illustrate the application of the triplet singularity method to a variety of wings and bodies in supersonic flow. Theoretical pressure coefficients are calculated using the isentropic pressure coefficient formula. The examples are compared with other theoretical methods and experimental data.

Parabolic Body of Revolution

Figures 4 and 5 give the axial pressure distribution on a parabolic body of revolution having a fineness ratio of 20 at $M = \sqrt{2}$. Comparisons between the triplet method and the surface source method of Reference 2 are shown for $\alpha = 0$ and 5° . For this smooth slender body, the two methods give very similar results, although a close examination shows small irregularities in the pressure distribution calculated by the source method caused by internal wave reflections.

Cone-Cylinder-Cone

A more severe test case was provided by a 15° cone-cylinder-cone body at $M = 2.0$. In this example, the surface source panel method of Reference 2 fails to give a convergent solution. Figures 6 and 7 show the axial pressure distribution at $\alpha = 0$ and 5° , respectively, compared to that obtained by the classical Karman-Moore method. (The Karman-Moore method uses a distribution of line sources and doublets along the axis, together with tangency boundary conditions on the body surface, Ref. 6.) The results of these two methods agree closely, indicating that the triplet method was effectively eliminated the strong internal waves that caused the source method to diverge. Figure 8 shows the circumferential pressure distribution on the 15° cone at $M = 2.0$ and $\alpha = 10^\circ$, on a section just behind the shoulder of the cone-cylinder and on a section of the cylinder extended 35 diameters behind the shoulder. The pressure distribution on this last section is seen to approach the incompressible cross-flow on a circular cylinder in two dimensions.

Nacelle with Internal Flow

The exterior pressure distribution on a circular nacelle with internal flow has been calculated at $M = \sqrt{2}$ for $\alpha = 0$ and 10° . The results are presented on Figure 9. This example again indicates the effectiveness of the triplet singularity in suppressing spurious internal waves, and can be compared with the nacelle results presented in Reference 1.

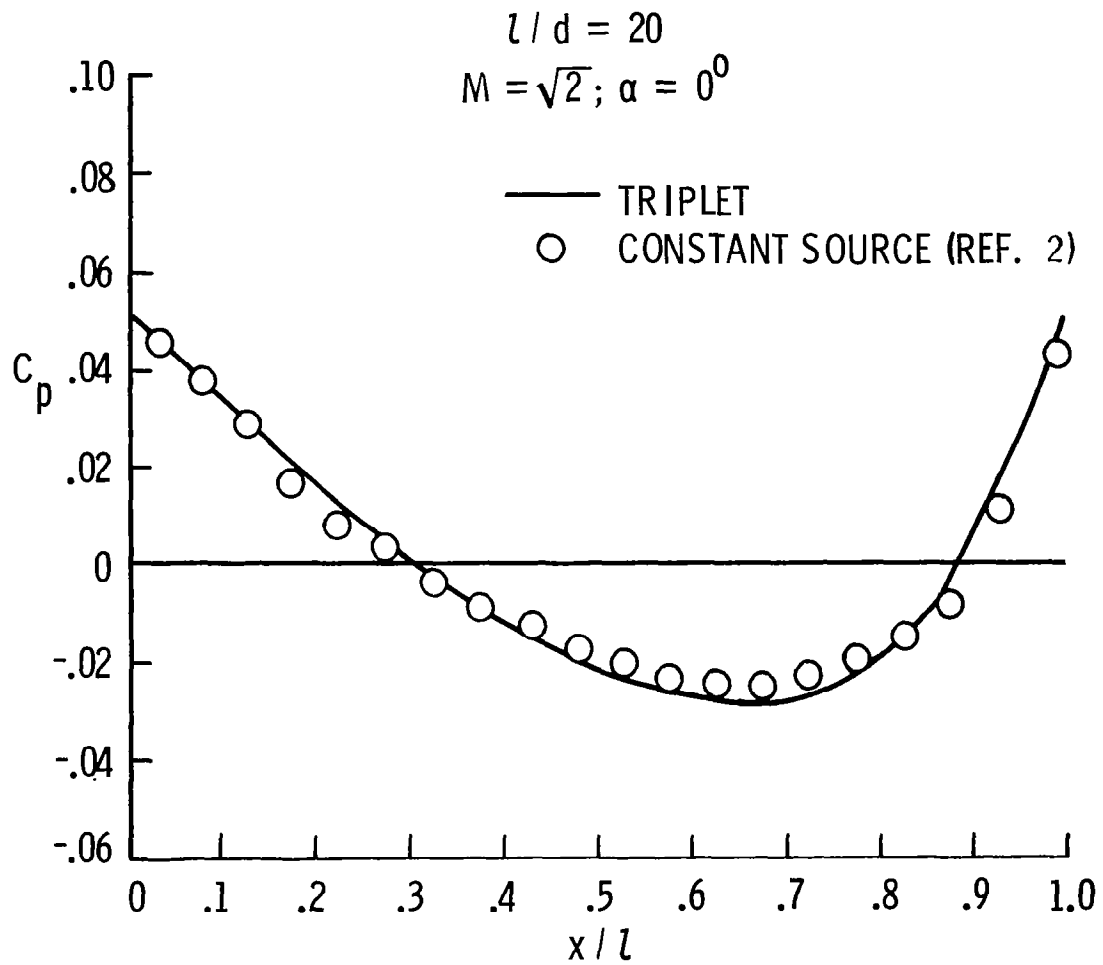


Figure 4. Parabolic Body: $\alpha = 0$ Degrees.

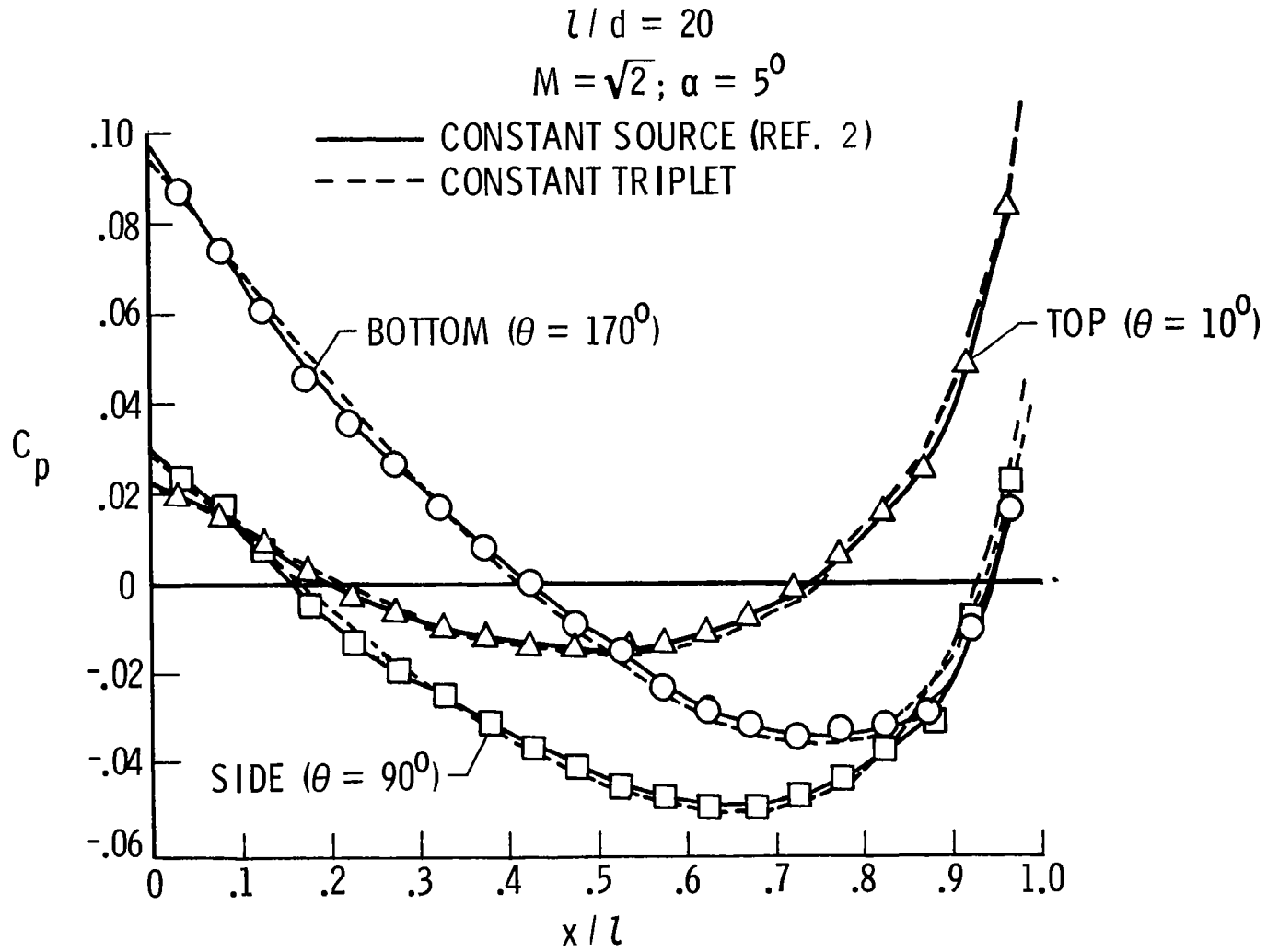


Figure 5. Parabolic Body; $\alpha = 5$ Degrees.

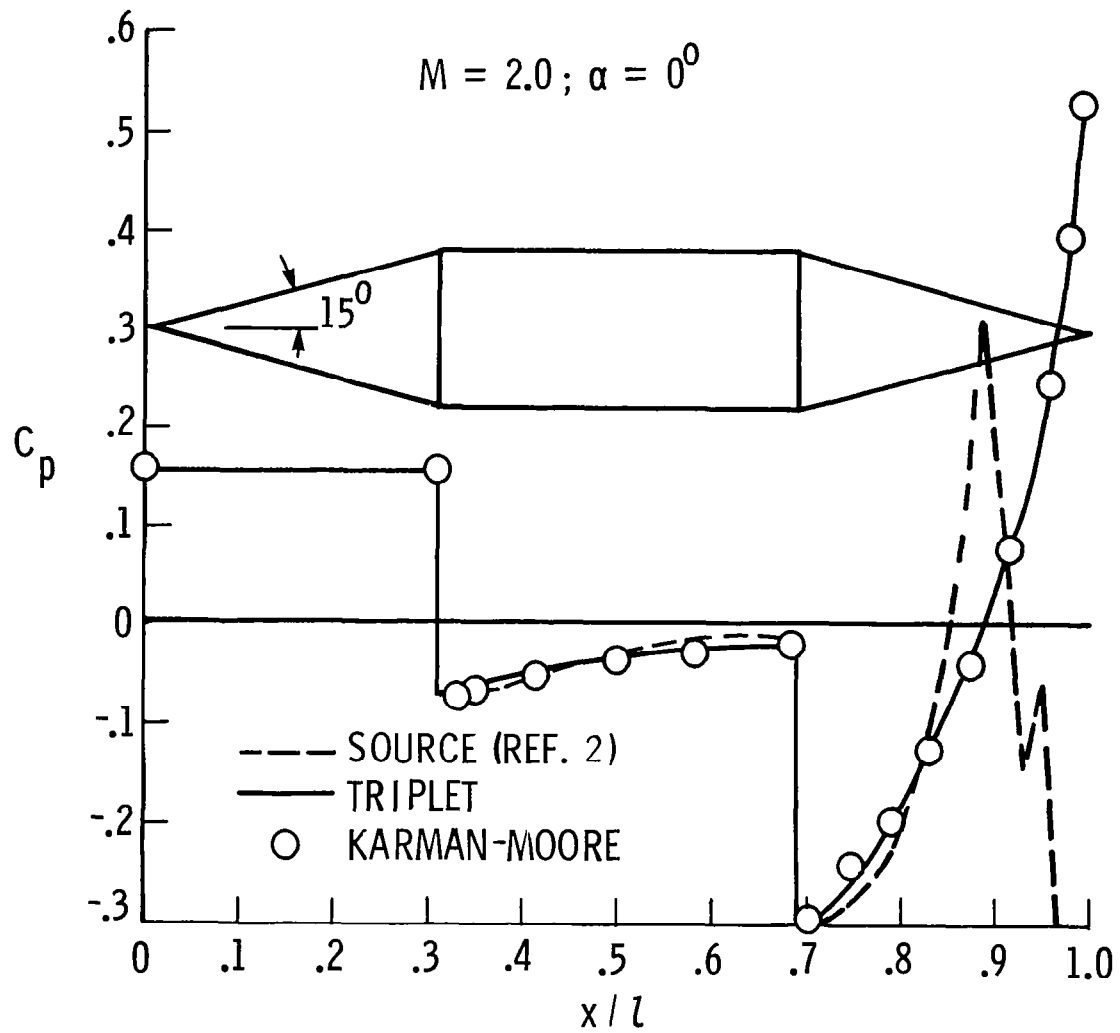


Figure 6. Cone-Cylinder-Cone; $\alpha = 0$ Degrees.

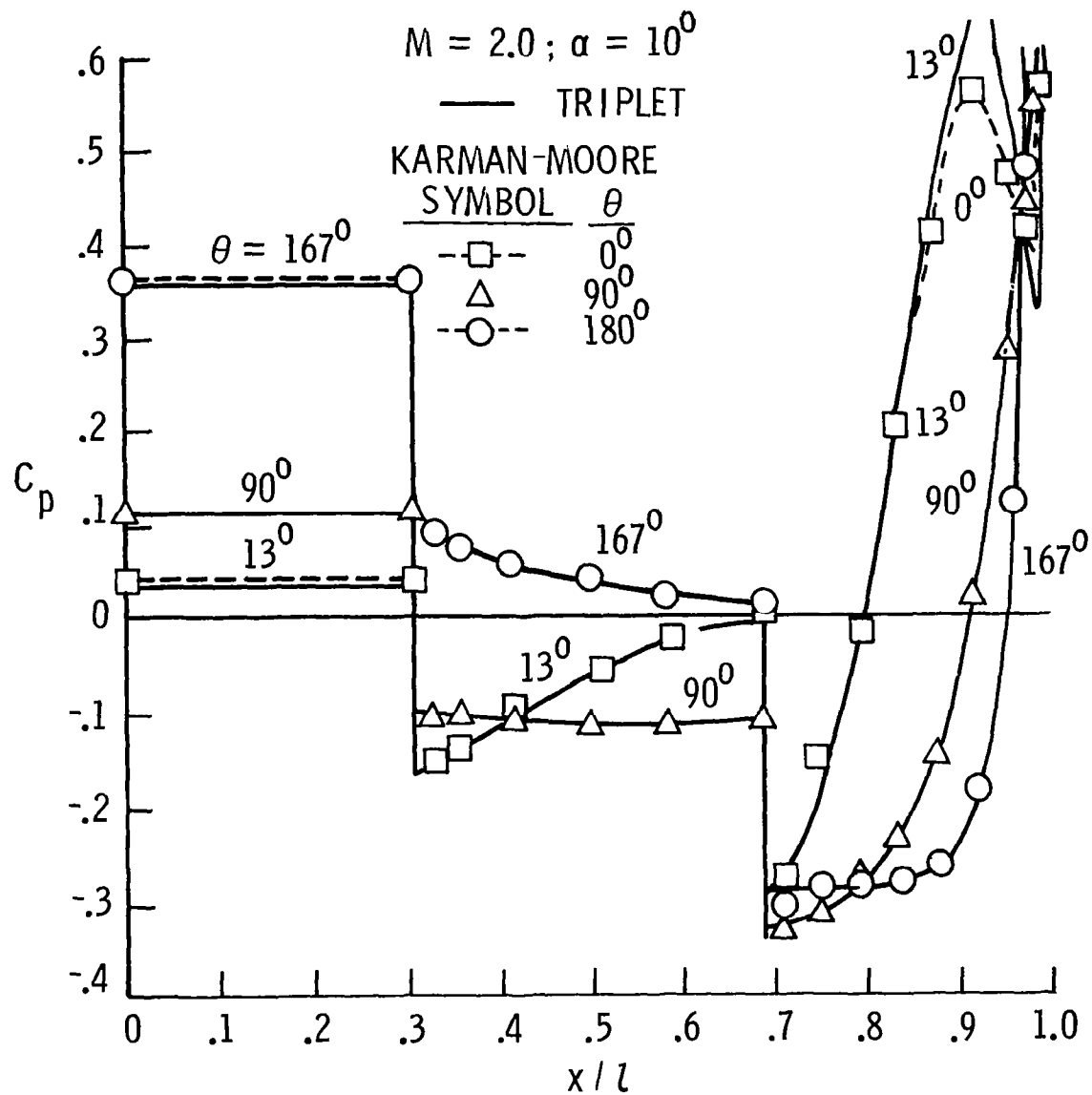


Figure 7. Cone-Cylinder-Cone; $\alpha = 10$ Degrees.

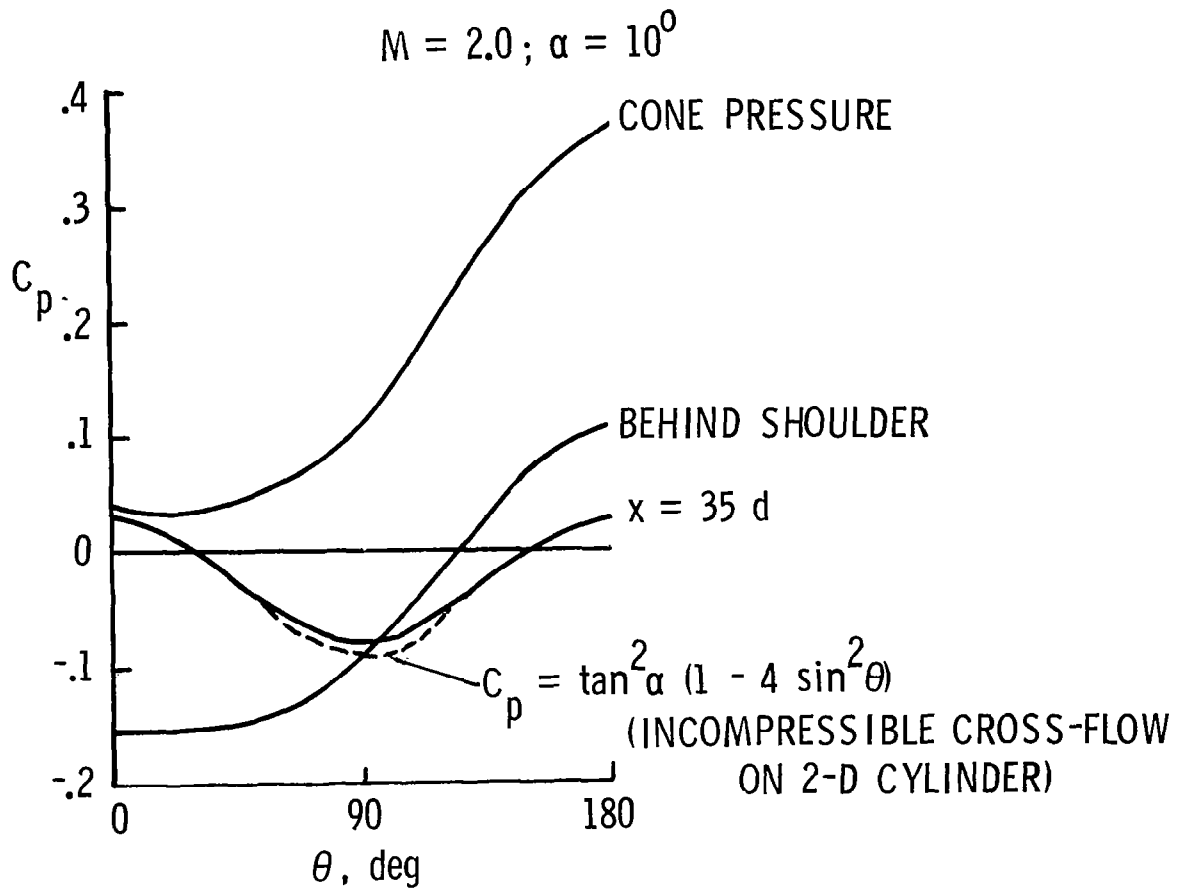


Figure 8. Circumferential Pressure on 15° Cone-Cylinder.

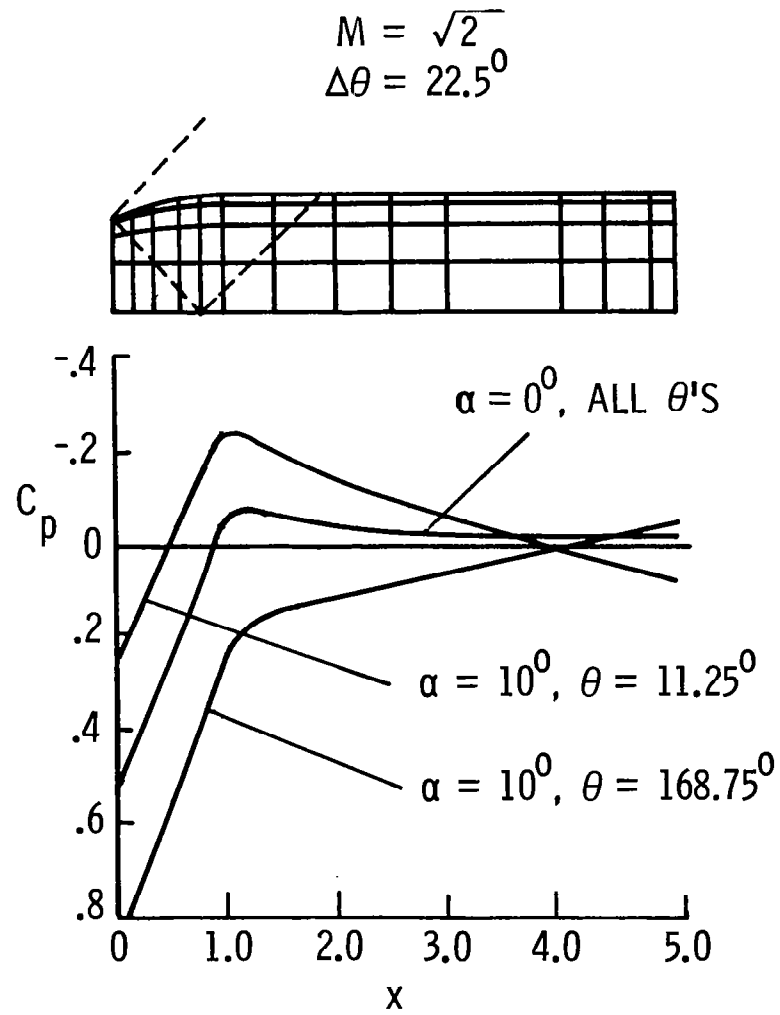


Figure 9. Nacelle Pressure Distribution.

Ogive-Cylinder-Boattail

Figures 10 and 11 give the axial pressure distribution on an ogive-cylinder-boattail body at $M = 2.3$. For $\alpha = 0^\circ$, Figure 10, a comparison is made between the triplet method and the experimental data of Reference 7. The theory tends to underestimate the pressure on the nose of the body, but agrees well with the data elsewhere, except on the boattail where viscous effects dominate. The underestimation of the nose pressure is a result of applying the linearized potential flow equations and tangency boundary conditions. A better approximation to the pressure on the nose can be obtained by applying a local Mach number correction described in Reference 4. The improvement is indicated by the dashed line on the figure.

For $\alpha = 4^\circ$, Figure 11, a comparison is made among the triplet method, the finite-difference method, Reference 8, and experimental data. The finite-difference method agrees well with the experimental data except on the boattail, while the triplet method again underestimates the pressure on the nose. No local Mach number correction has been added to the triplet results in this case.

Elliptic Cone

The triplet singularity may also be applied to the analysis of non-circular bodies. In Figure 12, the circumferential pressure distribution on an elliptic cone at $M = 1.89$ is compared with experimental data, Reference 9. For $\alpha = 0^\circ$, the theory overestimates the pressure slightly. For $\alpha = 6^\circ$, a more pronounced overestimation occurs on the lower surface.

B-1 Forebody

The pressure distributions along the upper and lower meridians of the B-1 forebody for $M = 2.2$ and $\alpha = 3^\circ$ are shown on Figure 13. Results from the triplet method are compared with the finite-difference method and experimental data obtained from Ref. 10. The finite-difference method agrees exceptionally well with the experimental data in this example. On the other hand, the triplet method underestimates the pressure on the nose cone, and fails to predict the pressure peak behind the canopy shock. This result is due to the shortcomings of linearized potential flow theory and can only be partially offset by applying a local Mach number correction.

Uncambered Arrow Wing

The pressure distribution calculated for an uncambered arrow wing having 70° sweepback and a 3 percent biconvex section at $M = 2.05$ and $\alpha = 4^\circ$ is presented on Figure 14. The results are compared with experimental data from

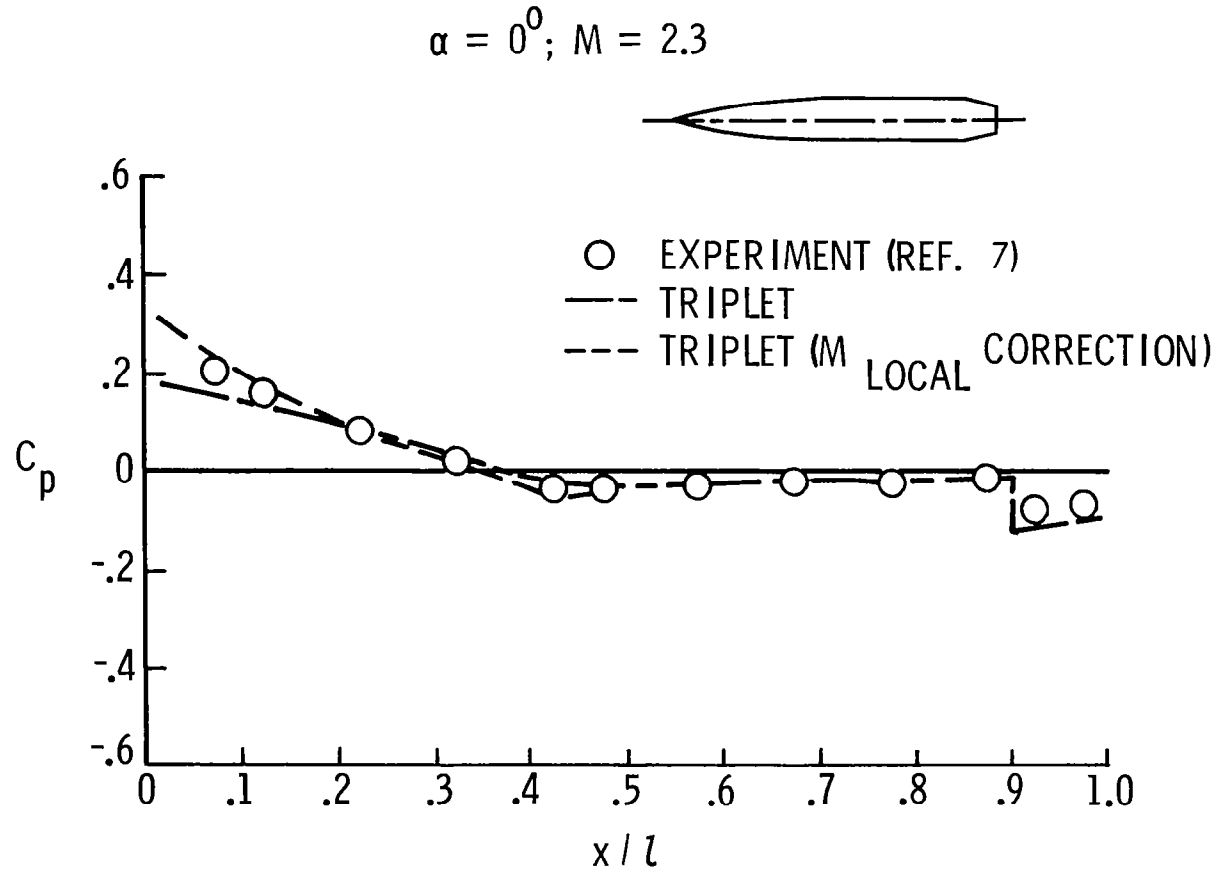


Figure 10. Ogive-Cylinder-Roattail; $\alpha = 0$ Degrees.

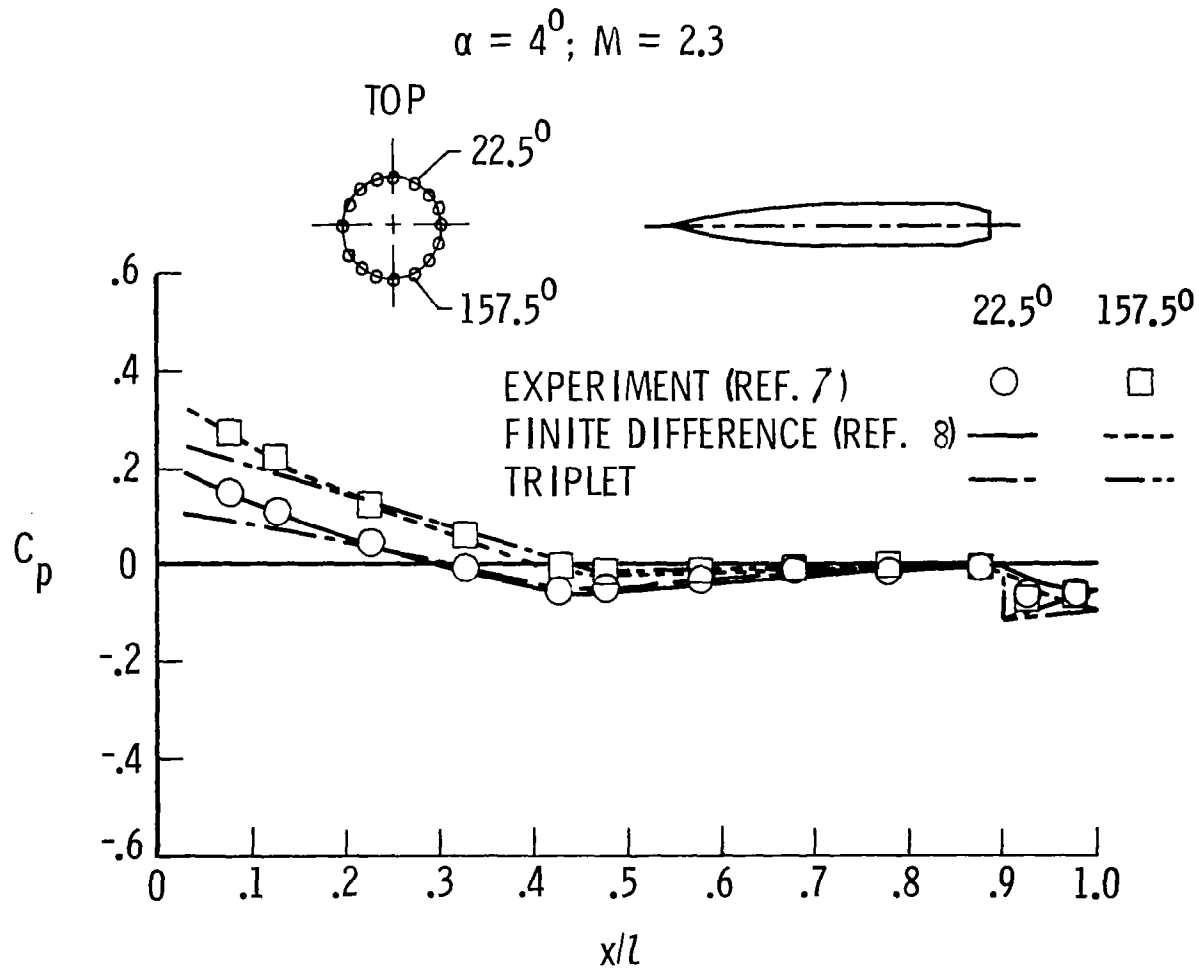


Figure 11. Ogive-Cylinder-Boattail; $\alpha = 4$ Degrees.

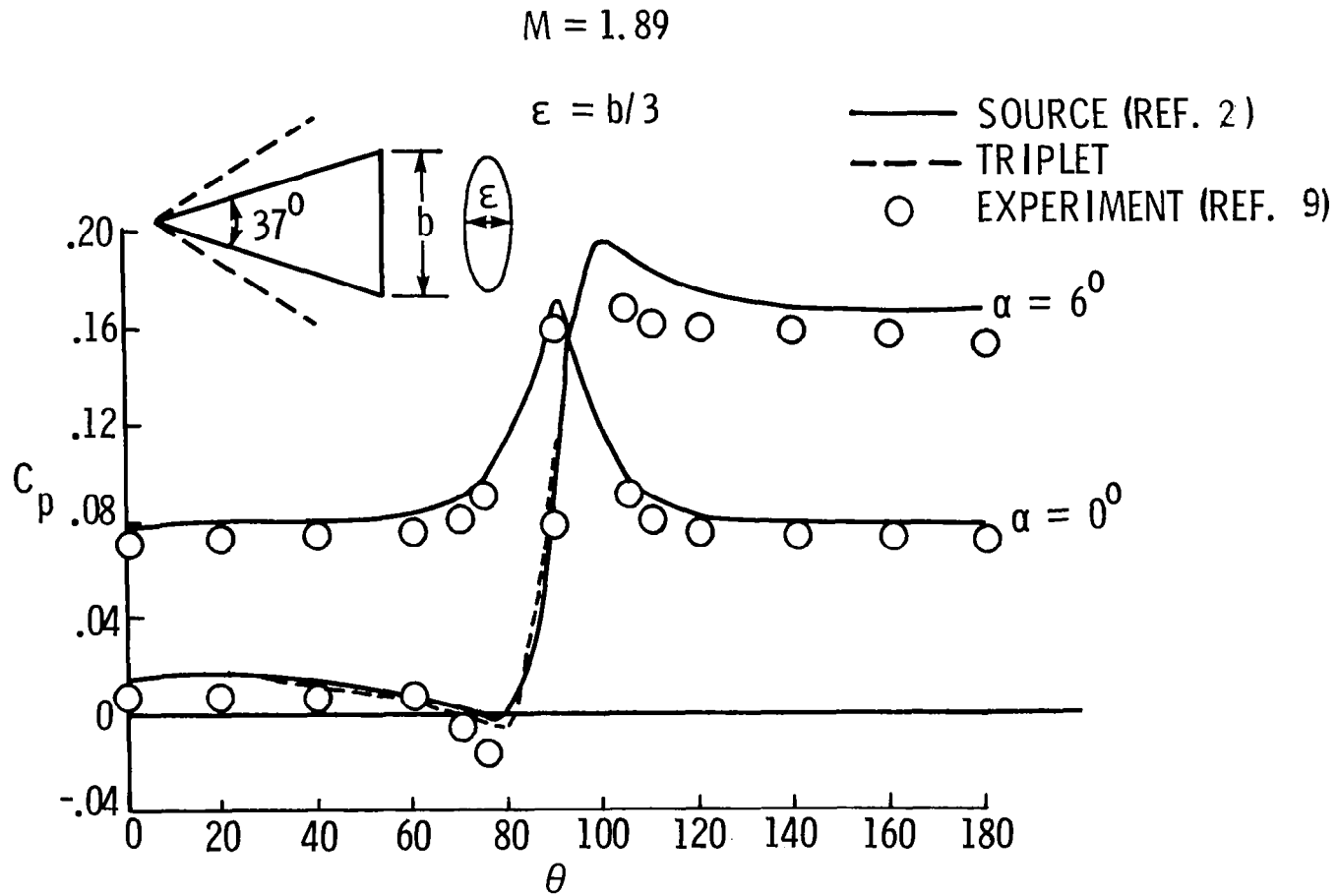


Figure 12. Elliptic Cone.

$M = 2.2; \alpha = 3^\circ$

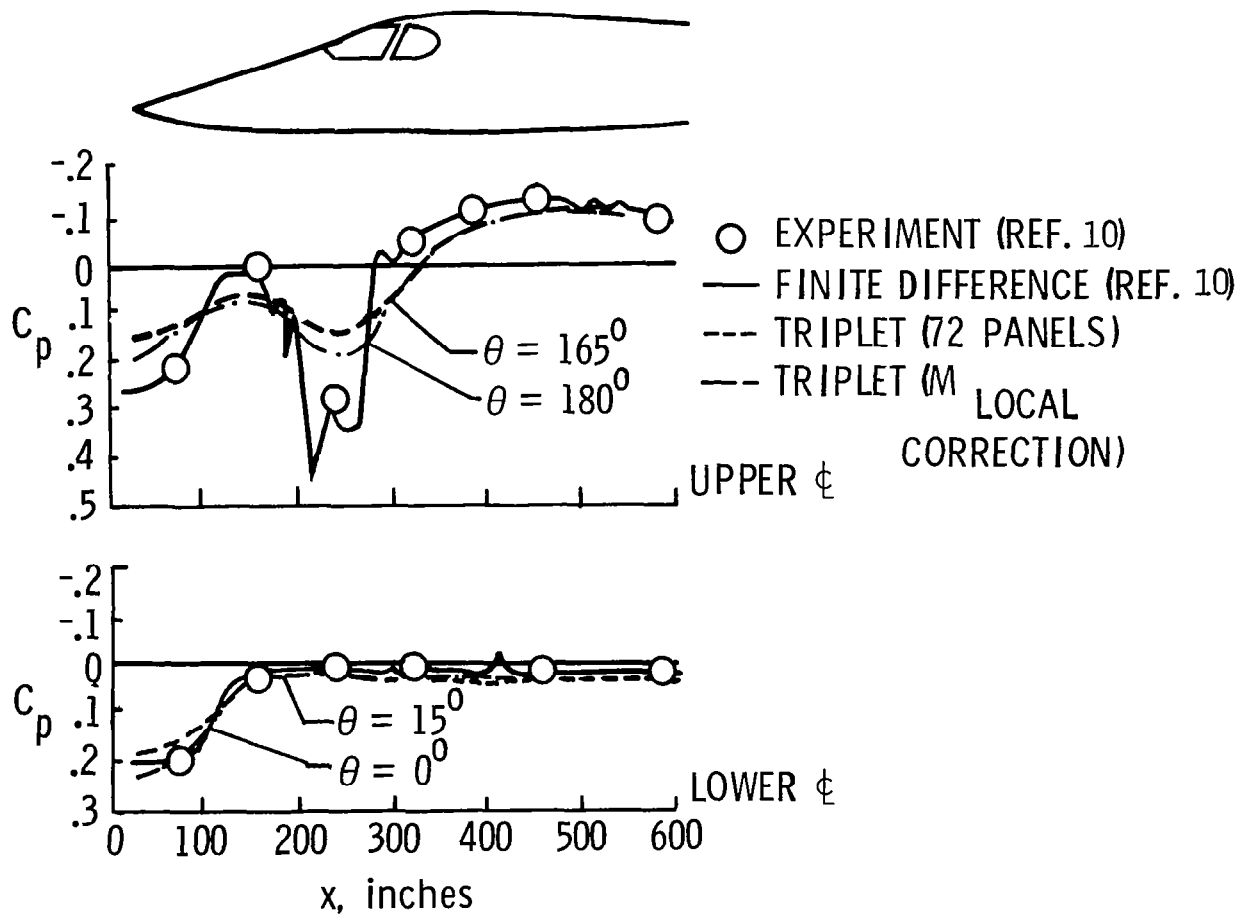


Figure 13. B-1 Forebody.

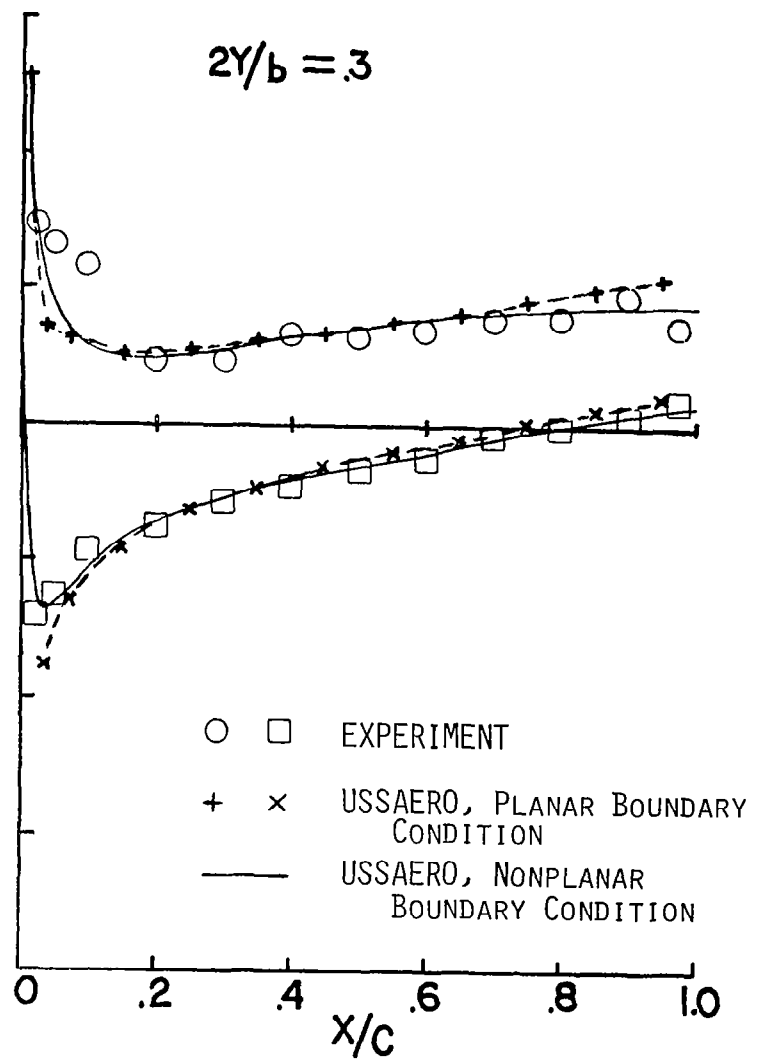
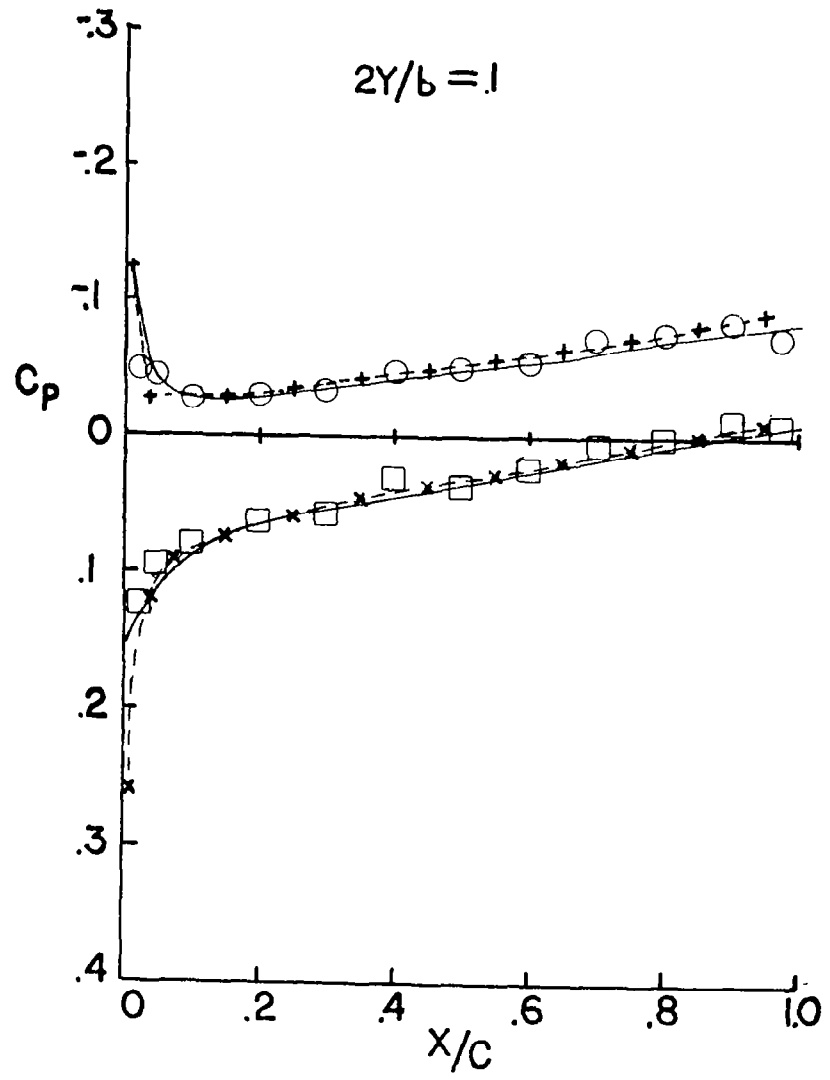


Figure 14. Uncambered Arrow Wing; $M = 2.05$, $\alpha = 4$ Degrees.

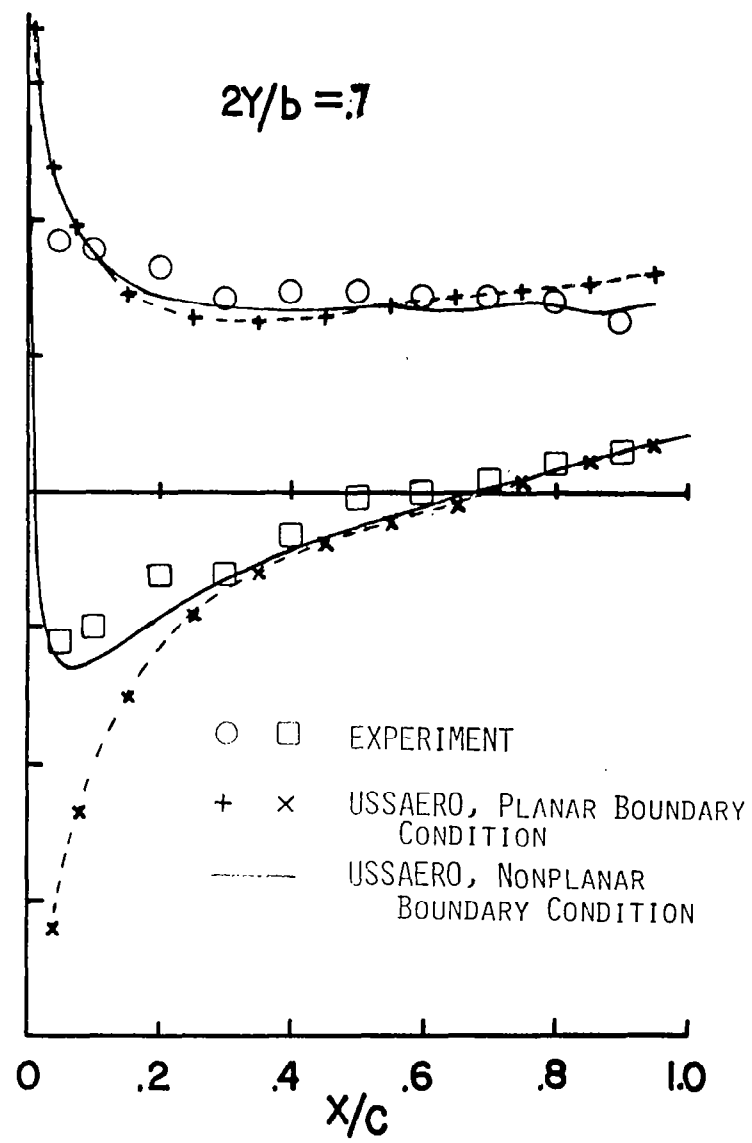
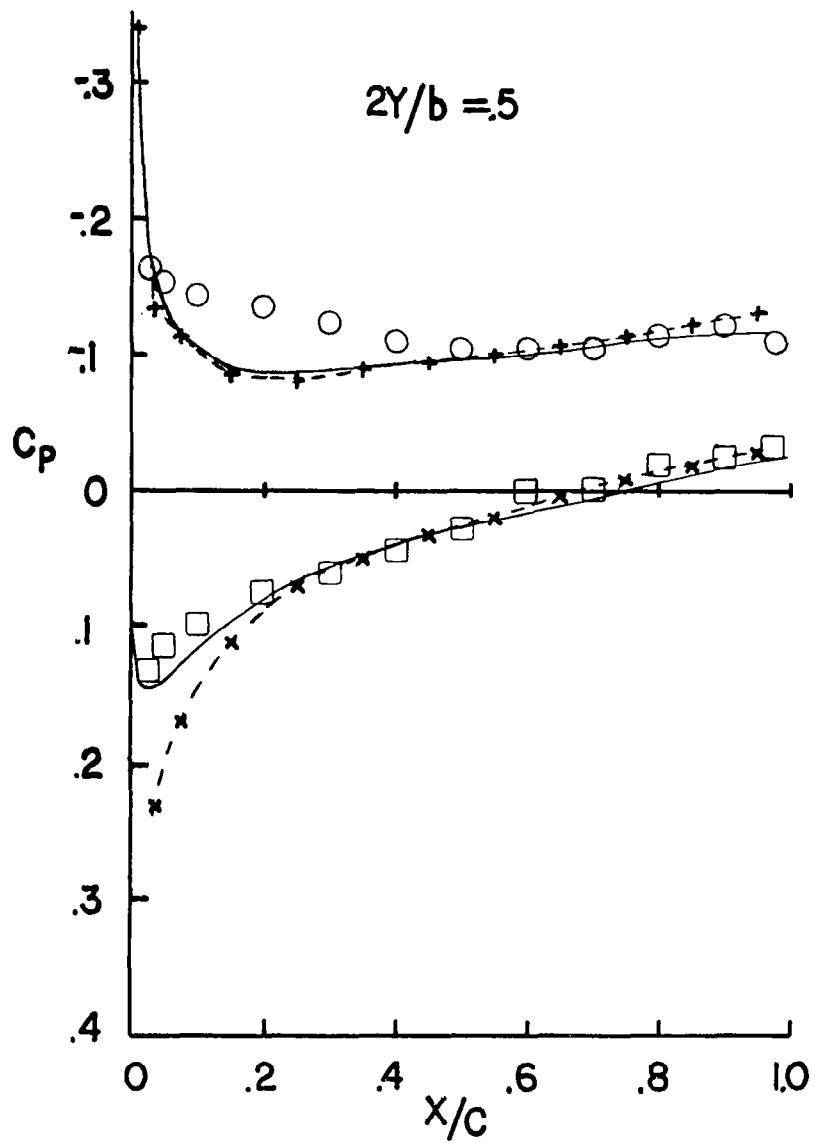


Figure 14. Continued.

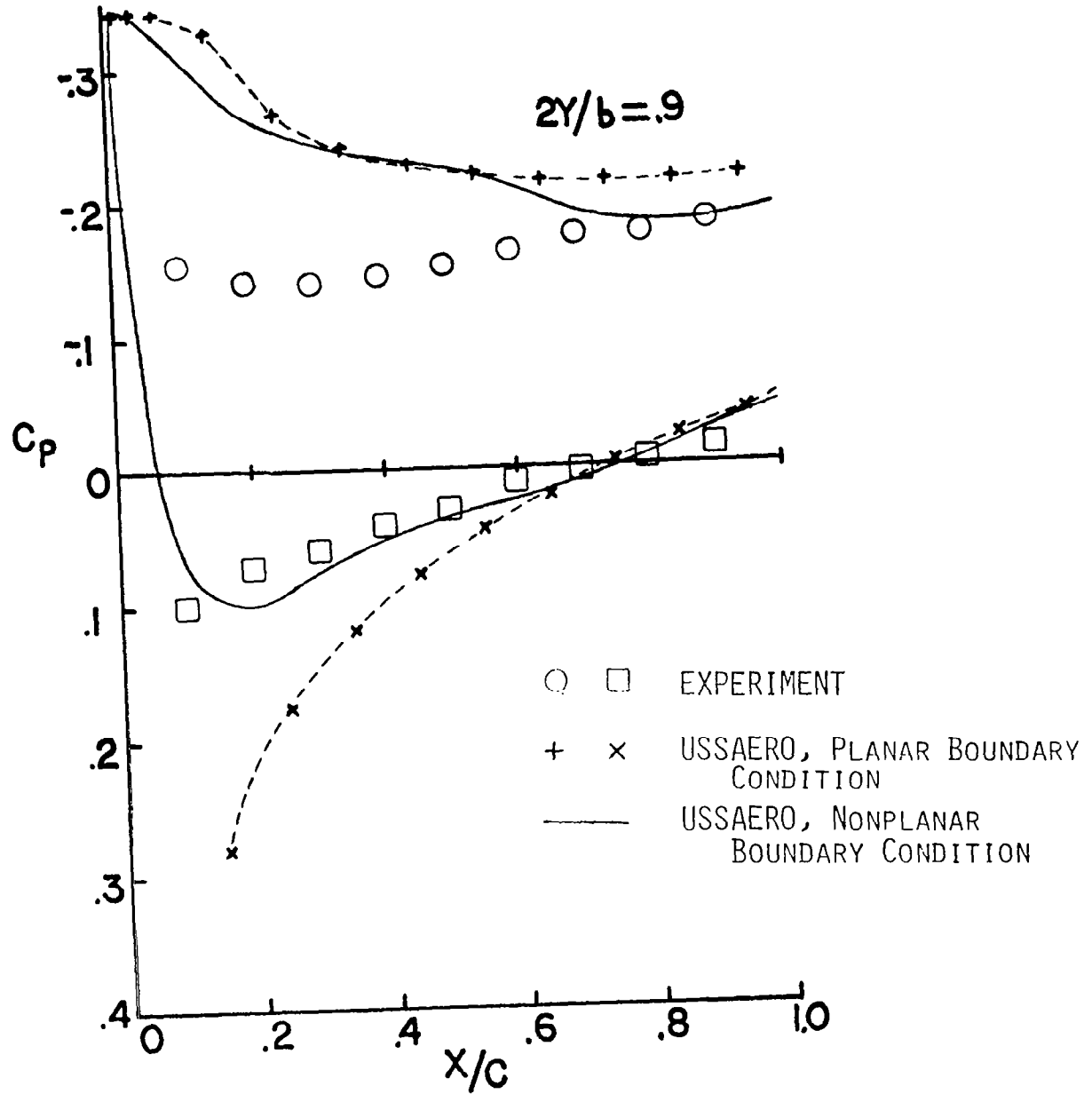


Figure 14. Concluded.

Reference 11, and a previous USSAERO calculation using planar boundary conditions with linearized pressure coefficient formula.

This wing has a subsonic leading edge and a supersonic trailing edge, and consequently uses a combination of linear vorticity and constant sources ahead of the sonic generator line, and constant triplets aft of that line. The results are smooth and are generally in good agreement with experimental data except on the upper surface near the wing tip. The theory also fails to predict the development of a small vortex above the leading edge on the in-board sections. The nonplanar boundary condition applied in this example gives a noticeable improvement in the pressure distribution on the lower surface, compared with the previous planar boundary condition calculation. However, much of this improvement is due to the use of the full isentropic pressure coefficient formula rather than to the particular aerodynamic model employed.

Cambered Arrow Wing

Figure 15 gives the pressure distribution calculated for a cambered and twisted arrow wing having the same planform and airfoil section as the previous example. The camber and twist was selected to give a design lift coefficient of .08 at $M = 2.05$ (see Ref. 11). The theory is compared with experimental data for $\alpha = 4^\circ$, and also with a previous USSAERO calculation using the planar boundary condition option.

In this calculation, the effect of the camber and twist was obtained by analyzing the equivalent uncambered wing in a nonuniform onset flow consisting of the normal component of the free stream velocity, plus an incremental normal velocity proportional to the slope of the chordwise camber distribution. The boundary condition of tangential flow is then applied at the upper and lower surface control points on the equivalent uncambered wing. This is consistent with the technique used to add camber effects in the planar boundary condition option of the USSAERO program.

The resulting chordwise pressure distributions are in reasonable agreement with the experimental data, except on the lower surface near the wing tip. Again, the nonplanar boundary condition calculations agree more closely with the lower surface experimental data than the previous planar boundary condition calculations, due primarily to the pressure coefficient formula employed.

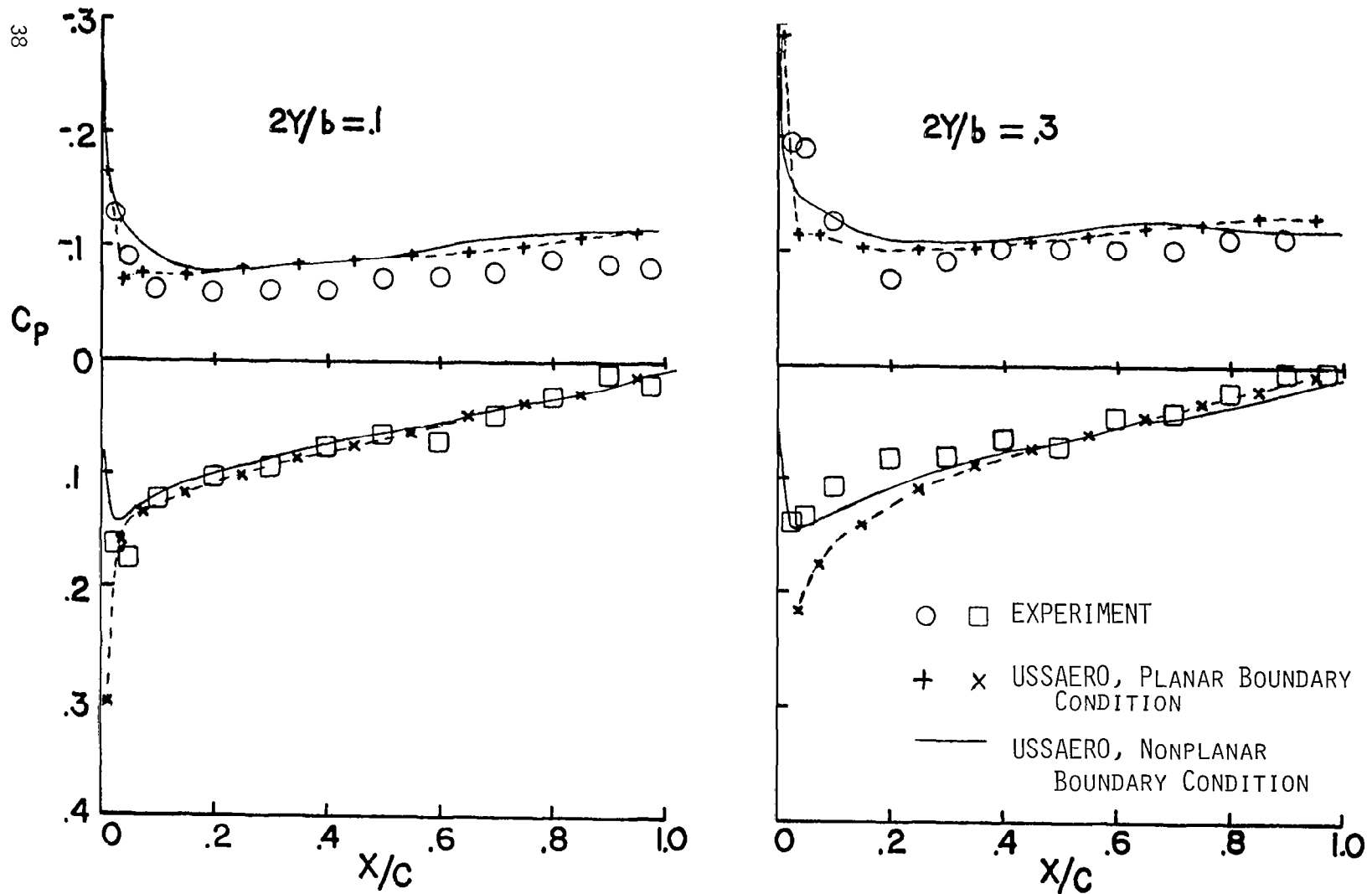


Figure 15. Cambered Arrow Wing; $M = 2.05$, $\alpha = 4$ Degrees.

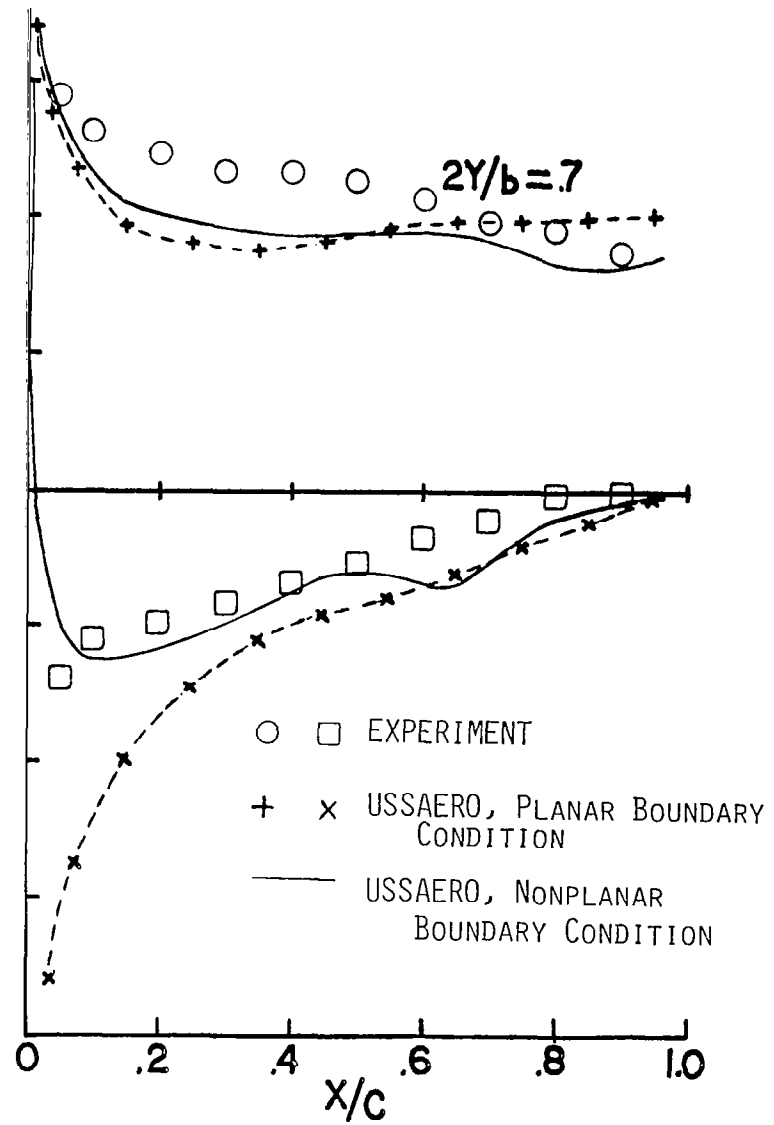
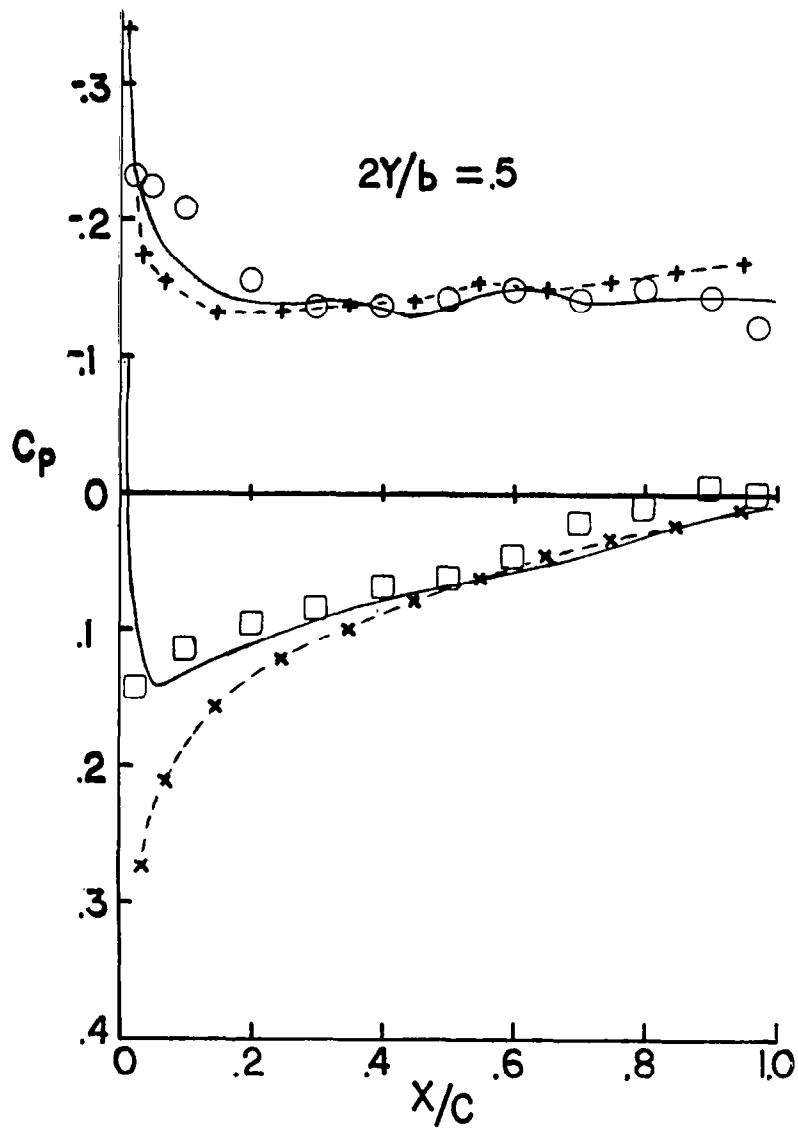


Figure 15. Continued.

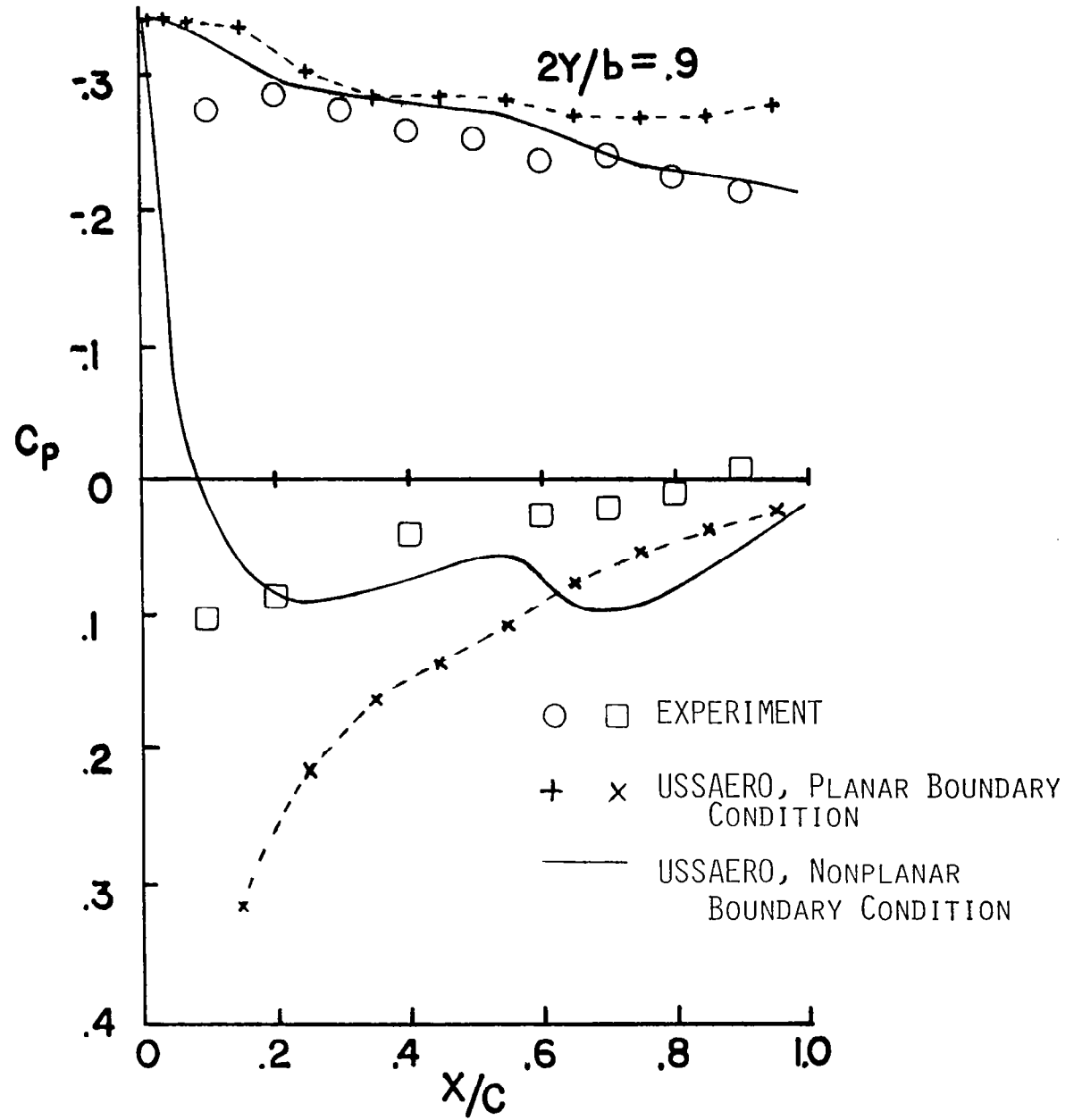


Figure 15. Concluded.

CONCLUSIONS

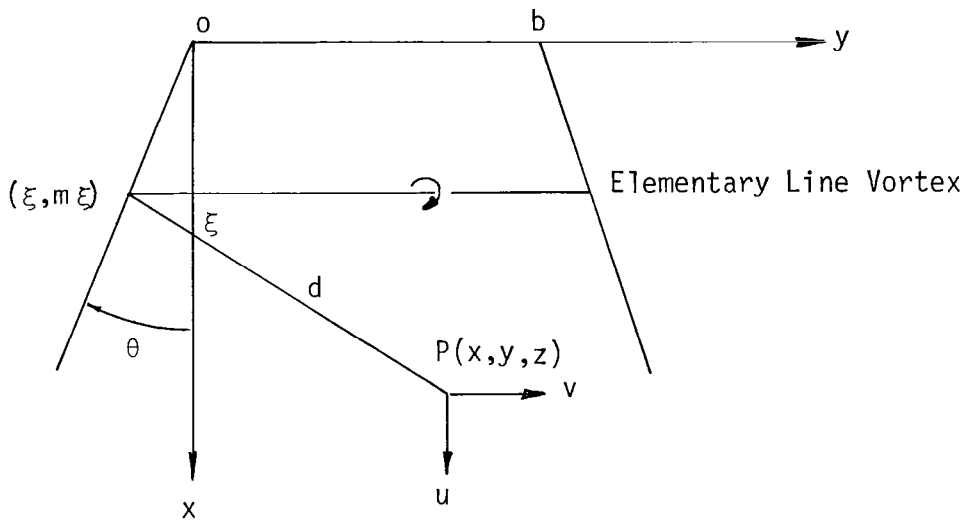
A triplet singularity has been developed and applied to the analysis of wings and bodies in supersonic flow. The new singularity has been found most effective in the analysis of bodies, and appears to eliminate any sensitivity of the surface pressure to the details of the panelling.

The new singularity also makes it possible to extend the method to the analysis of wings defined by surface panels, using nonplanar boundary conditions in supersonic flow. However, no significant improvement in the prediction of the wing pressure distribution has resulted from this extension. It is concluded that a more extensive evaluation of the method is required to determine if the overall improvements obtained justify the additional numerical complexity involved.

APPENDIX A: DERIVATION OF BODY SINGULARITIES

1. Circumferential Vortex Distribution

The incompressible velocity components induced at a point, P, by a constant vortex distribution in the plane of the panel are derived by integrating the influences of a series of elementary line vortices extending across the panel parallel to the leading edge. The geometry of an elementary line vortex located at a distance, ξ , from the leading edge and having strength, $d\xi$, is illustrated below.



The panel lies in the x,y plane and the edge slope, $m = \tan \theta$, is an arbitrary constant. The distance from the point, P, to the left end of the elementary vortex is

$$d = \sqrt{(x - \xi)^2 + (y - m\xi)^2 + z^2}$$

The velocity components are obtained by applying a 90 degree coordinate rotation to the line vortex velocity formulas given by equations (6) through (8) of Reference 2, and integrating across the panel as follows.

$$u_{V_c} = -z \int \frac{(y - m\xi) d\xi}{((x - \xi)^2 + z^2) \sqrt{(x - \xi)^2 + (y - m\xi)^2 + z^2}} \quad (A1)$$

$$v_{V_c} = 0 \quad (A2)$$

$$w_{V_c} = \int \frac{(x - \xi)(y - m\xi) d\xi}{((x - \xi)^2 + z^2) \sqrt{(x - \xi)^2 + (y - m\xi)^2 + z^2}} \quad (A3)$$

Put $v = x - \xi$. Then

$$u_{V_c} = z \left[(y - mx) J_1 + mJ_2 \right] \quad (A4)$$

$$w_{V_c} = mz^2 J_1 - (y - mx) J_2 - mK_1 \quad (A5)$$

where

$$J_1 = \int \frac{dv}{(v^2 + z^2) \sqrt{av^2 + 2bv + c}} \quad (A6)$$

$$J_2 = \int \frac{v dv}{(v^2 + z^2) \sqrt{av^2 + 2bv + c}} \quad (A7)$$

$$K_1 = \int \frac{dv}{\sqrt{av^2 + 2bv + c}} \quad (A8)$$

The integrals, J_1 and J_2 , are given in Appendix I of Reference 2, and the integral K_1 is in standard form. Evaluating these integrals, the three components of velocity induced by the inboard corner of the panel can be written:

$$u_{V_C} = \tan^{-1} \frac{z\sqrt{x^2 + y^2 + z^2}}{-x(y - mx) + mz^2} \quad (A9)$$

$$v_{V_C} = 0 \quad (A10)$$

$$w_{V_C} = \sinh^{-1} \frac{y}{\sqrt{x^2 + z^2}} - \frac{m}{\sqrt{1 + m^2}} \sinh^{-1} \frac{x + my}{\sqrt{(y - mx)^2 + (1 + m^2) z^2}} \quad (A11)$$

The compressible velocity components can be obtained from the above expressions by applying the extended Gothert's rule. In supersonic flow, with $\beta = \sqrt{M^2 - 1}$,

$$u_{V_C} = F = \tan^{-1} \frac{z\sqrt{x^2 - \beta^2(y^2 + z^2)}}{-x(y - mx) - m\beta^2 z^2} \quad (A12)$$

$$v_{V_C} = 0 \quad (A13)$$

$$w_{V_C} = \beta \left[\frac{\beta m}{\sqrt{1 - \beta^2 m^2}} \cosh^{-1} \frac{x - \beta^2 my}{\beta \sqrt{(y - mx)^2 + (1 - \beta^2 m^2) z^2}} - \sin^{-1} \frac{\beta y}{\sqrt{x - \beta^2 z^2}} \right] = \beta (\beta m G - H) \quad (A14)$$

2. Circumferential Source Distribution

The incompressible velocity components induced at a point by a constant source distribution in the plane of the panel are given by Eqns. (18) through (20) of Reference 2. In supersonic flow, these expressions become:

$$u_{SC} = - (\beta m G - H) / \beta \quad (A15)$$

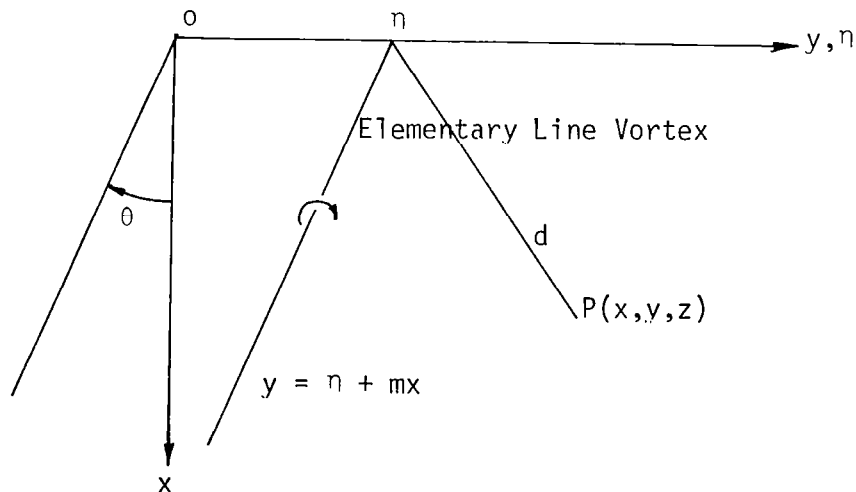
$$v_{SC} = G \quad (A16)$$

$$w_{SC} = -F \quad (A17)$$

where F, G, and H are defined above.

3. Edge Vortex Distribution

The incompressible velocity components induced at a point by a constant vortex distribution oriented parallel to the side edge of the panel are derived by integrating the influence of elementary line vortices across the panel in the spanwise direction. The geometry is illustrated below.



The panel lies in the x,y plane, and the edge slope, $m = \tan \theta$, is an arbitrary constant. The distance from the point, P, to the origin of the vortex is

$$d = \sqrt{x^2 + (y - \eta)^2 + z^2}$$

The velocity components are obtained by rotating the line vortex velocity formulas given by equations (6) through (8) of Reference 2 through the angle, θ , and integrating across the panel as follows:

$$u_{VE} = mz \int \frac{x + m(y - \eta) d\eta}{[(y - mx - \eta)^2 + (1+m^2)z^2] \sqrt{x^2 + (y - \eta)^2 + z^2}} \quad (A18)$$

$$v_{VE} = -u/m \quad (A19)$$

$$w_{VE} = \int \frac{(y - mx - \eta)(x + m(y - \eta)) d\eta}{[(y - mx - \eta)^2 + (1+m^2)z^2] \sqrt{x^2 + (y - \eta)^2 + z^2}} \quad (A20)$$

These integrals can be expressed in terms of the J and K integrals by substituting $v = y - mx - \eta$. Performing the integrations, the three components of velocity induced by the inboard corner of the panel may be written:

$$u_{VE} = -m \tan^{-1} \frac{z \sqrt{x^2 + y^2 + z^2}}{-x(y - mx) + mz^2} \quad (A21)$$

$$v_{VE} = -u/m \quad (A22)$$

$$w_{VE} = \sqrt{1 + m^2} \sinh^{-1} \frac{x + my}{\sqrt{(y - mx)^2 + (1 + m^2)z^2}}$$

$$- m \sinh^{-1} \frac{y}{\sqrt{x^2 + z^2}} + m \log \sqrt{x^2 + z^2} \quad (A23)$$

These formulas can also be obtained by performing a 90° coordinate rotation in Eqns. (43) through (45) of Reference 2. , In supersonic flow,

$$u_{VE} = -mF \quad (A24)$$

$$v_{VE} = F \quad (A25)$$

$$w_{VE} = (1 - \beta^2 m^2)G + \beta mH \quad (A26)$$

where F, G, and H are defined by Eqns. (A12) through (A14).

4. Edge Source Distribution

The corresponding edge source distribution can be obtained by multiplying the circumferential source distribution by $-m$. In supersonic flow,

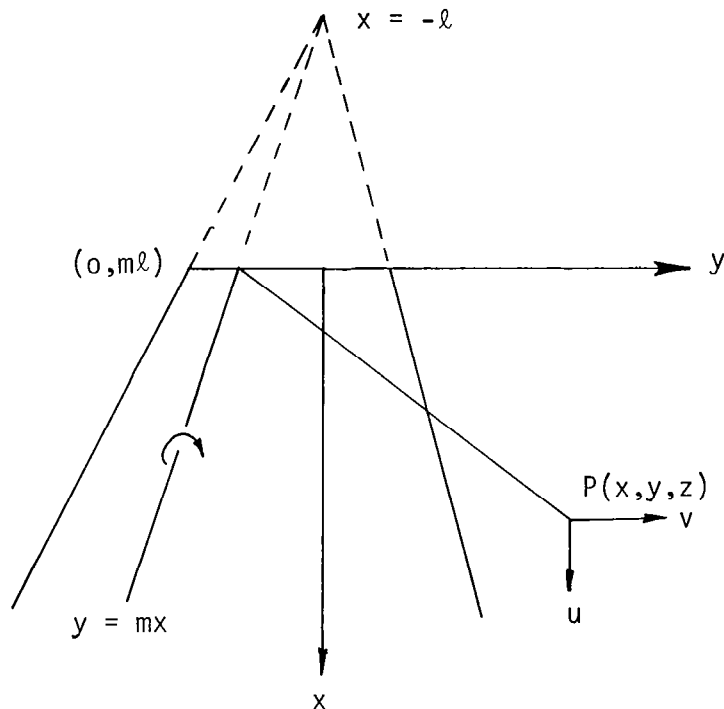
$$u_{SE} = m(\beta mG - H)/\beta \quad (A27)$$

$$v_{SE} = -mG \quad (A28)$$

$$w_{SE} = mF \quad (A29)$$

5. Radial Vortex Distribution

In the radial vortex distribution, the velocity components at a point are obtained by integrating the influences of a series of elementary line vortices lying along radial lines from an apex defined by the intersection of the two side edges. The geometry is illustrated below.



The elementary line vortex lies along the line, $y = mx$, and originates at the point, $0, m\ell$, where ℓ is the distance of the apex ahead to the panel leading edge. The distance from the point, P , to the origin of the vortex is

$$D = \sqrt{x^2 + (y - m\ell)^2 + z^2}$$

In this case, the vortex inclination, $m = \tan \theta$, varies from m_1 to m_2 across the panel. The velocity components are obtained by rotating the line vortex velocity formulas given by Eqns. (6) through (8) of Reference 2 through the angle, θ , and integrating with respect to m as follows:

$$u_{VR} = z\ell \int_{m_1}^{m_2} \frac{[x + m(y - m\ell)]m \, dm}{[(y - m(x + \ell))^2 + (1 + m^2)z^2]\sqrt{x^2 + (y - m\ell)^2 + z^2}} \quad (A30)$$

$$v_{VR} = -z\ell \int_{m_1}^{m_2} \frac{x + m(y - m\ell) \, dm}{[(y - m(x + \ell))^2 + (1 + m^2)z^2]\sqrt{x^2 + (y - m\ell)^2 + z^2}} \quad (A31)$$

$$w_{VR} = - [(x + \ell)u + yv] / z \quad (A32)$$

Substituting $v = m + \frac{y(x + \ell)}{(x + \ell)^2 + z^2}$, the above integrals can be expanded into expressions containing the J integrals (with $\gamma = yz\ell/((x + \ell)^2 + z^2)$), and other integrals of standard form. Performing the integrations, the three components of velocity induced by the inboard corner of the panel may be written:

$$u_{VR} = \frac{-1}{(x + \ell)^2 + z^2} \left\{ z \left[D + \ell(x + \ell)G_R \right] + y\ell \frac{(x + \ell)^2 - z^2}{(x + \ell)^2 + z^2} F \right. \\ \left. + \frac{2yz\ell(x + \ell)}{(x + \ell)^2 + z^2} \left[yG_R - H \right] \right\} \quad (A33)$$

$$v_{VR} = \frac{\ell}{(x + \ell)^2 + z^2} \left\{ (x + \ell) F + z [yG_R - H] \right\} \quad (A34)$$

$$w_{VR} = \frac{1}{(x + \ell)^2 + z^2} \left\{ (x + \ell)(D + \ell(x + \ell)G_R) \right. \\ \left. + y\ell \frac{(x + \ell)^2 - z^2}{(x + \ell)^2 + z^2} (yG_R - H) - \frac{2yz\ell(x + \ell)}{(x + \ell)^2 + z^2} F \right\} \quad (A35)$$

where $F = \tan^{-1} \frac{zD}{-x(y - m(x + \ell)) + mz^2}$ (A36)

$$G_R = \frac{1}{D_R} \sinh^{-1} \frac{x(x + \ell) + y(y - m\ell) + z^2}{\ell \sqrt{(y - m(x + \ell))^2 + (1 + m^2)z^2}} \quad (A37)$$

$$H = \sinh^{-1} \frac{y - m\ell}{\sqrt{x^2 + z^2}} \quad (A38)$$

and $D = \sqrt{x^2 + (y - m\ell)^2 + z^2}$,

$$D_R = \sqrt{(x + \ell)^2 + y^2 + z^2}$$

In supersonic flow,

$$u_{VR} = \frac{-1}{(x + \ell) - \beta^2 z^2} \left\{ z(D + \ell(x + \ell)G_R) + y\ell \frac{(x + \ell)^2 + \beta^2 z^2}{(x + \ell)^2 - \beta^2 z^2} F \right. \\ \left. - \frac{2\beta y z \ell (x + \ell)}{(x + \ell)^2 - \beta^2 z^2} (yG_R - H) \right\} \quad (A39)$$

$$v_{VR} = \frac{\ell}{(x + \ell)^2 - \beta^2 z^2} \left\{ (x + \ell)F - \beta z(\beta y G_R - H) \right\} \quad (A40)$$

$$w_{VR} = \frac{1}{(x + \ell)^2 - \beta^2 z^2} \left\{ (x + \ell)(D + \ell(x + \ell)G_R) \right. \\ \left. - \beta y \ell \frac{(x + \ell)^2 + \beta^2 z^2}{(x + \ell)^2 - \beta^2 z^2} (\beta y G_R - H) + \frac{2\beta^2 y z \ell (x + \ell)}{(x + \ell)^2 - \beta^2 z^2} F \right\} \quad (A41)$$

where $F = \tan^{-1} \frac{zD}{-x(y - m(x + \ell)) - \beta^2 m z^2}$ (A42)

$$G_R = \frac{1}{D_R} \cosh^{-1} \frac{x(x + \ell) - \beta^2 y(y - m\ell) - \beta^2 z^2}{\beta \ell \sqrt{(y - m(x + \ell))^2 + (1 - \beta^2 m^2)z^2}} \quad (A43)$$

$$H = \sin^{-1} \frac{y - m\ell}{\beta \sqrt{x^2 - \beta^2 z^2}} \quad (\text{A44})$$

and
$$D = \sqrt{x^2 - \beta^2(y - m\ell)^2 - \beta^2 z^2}$$

$$D_R = \sqrt{(x + \ell)^2 - \beta^2(y^2 + z^2)}$$

6. Radial Source Distribution

The derivation of the velocity components induced by a radial source distribution is similar to that used for the radial vortex distribution, with elementary line sources replacing the elementary line vortices along radial lines from the apex of the panel. The three components of velocity may be written in integral form as follows:

$$u_{SR} = \ell \int \frac{[xy - m(x(x + \ell) + z^2)] m^2 dm}{[(y - m(x + \ell))^2 + (1 + m^2)z^2] \sqrt{x^2 + (y - m\ell)^2 + z^2}} + \ell \int \frac{mdm}{\sqrt{x^2 + (y - m\ell)^2 + z^2}} \quad (\text{A45})$$

$$v_{SR} = -\ell \int \frac{[xy - m(x(x + \ell) + z^2)] m dm}{[(y - m(x + \ell))^2 + (1 - m^2)z^2] \sqrt{x^2 + (y - m\ell)^2 + z^2}} \quad (A46)$$

$$w_{SR} = -u_{VR} \quad (A47)$$

Carrying out the integrations, using the substitutions indicated in the previous section, the three components of velocity induced by the inboard corner of the panel in incompressible flow are:

$$u_{SR} = \frac{1}{(x + \ell)^2 + z^2} \left\{ (x + \ell)D + z^2 \ell G_R - \frac{2yz\ell(x + \ell)}{(x + \ell)^2 + z^2} F \right. \\ \left. + y\ell \frac{(x + \ell)^2 - z^2}{(x + \ell)^2 + z^2} (yG_R - H) \right\} \quad (A48)$$

$$v_{SR} = \frac{\ell}{(x + \ell)^2 + z^2} \left\{ zF - (x + \ell)(yG_R - H) \right\} - H \quad (A49)$$

$$w_{SR} = -u_{VR} \quad (A50)$$

where F , G_R , and H are defined by Eqns. (A36) through (A38).

In supersonic flow:

$$u_{SR} = \frac{1}{\beta^2 [(x + \ell)^2 - \beta^2 z^2]} \left\{ - (x + \ell)D - \beta^2 z^2 \ell G_R - \frac{2\beta^2 y z \ell (x + \ell)}{(x + \ell)^2 - \beta^2 z^2} F \right. \\ \left. + \beta y \ell \frac{(x + \ell)^2 + \beta^2 z^2}{(x + \ell)^2 - \beta^2 z^2} (\beta y G_R - H) \right\} \quad (A51)$$

$$v_{SR} = \frac{\ell}{\beta [(x + \ell)^2 - \beta^2 z^2]} \left\{ \beta z F - (x + \ell)(\beta y G_R - H) \right\} - \frac{H}{\beta} \quad (A52)$$

$$w_{SR} = -u_{VR} \quad (A53)$$

where u_{VR} is defined by Eqn. (A39), and F , G_R and H are defined by Eqns. (A42) through (A44).

7. Leading-Edge Line Vortex

In incompressible flow, the three components of velocity induced at a point, (x, y, z) , by a linearly varying line vortex located along the panel leading edge are:

$$u_{VL} = \frac{zd}{x^2 + z^2} \left(1 + \frac{y}{d} \right) \quad (A54)$$

$$v_{VL} = 0 \quad (A55)$$

$$w_{VL} = - \frac{xd}{x^2 + z^2} \left(1 + \frac{y}{d}\right) \quad (A56)$$

where $d = \sqrt{x^2 + y^2 + z^2}$

In supersonic flow,

$$u_{VL} = \frac{zd}{x^2 - \beta^2 z^2} \quad (A57)$$

$$v_{VL} = 0 \quad (A58)$$

$$w_{VL} = - \frac{xd}{x^2 - \beta^2 z^2} \quad (A59)$$

where $d = \sqrt{x^2 - \beta^2(y^2 + z^2)}$

8. Leading-Edge Line Source

In incompressible flow, the three components of velocity induced at a point, (x,y,z) by a linearly varying line source located along the panel leading edge are:

$$u_{SL} = - \frac{xd}{x^2 + z^2} \quad (A60)$$

$$v_{SL} = \sinh^{-1} \frac{y}{\sqrt{x^2 + z^2}} \quad (A61)$$

$$w_{SL} = - \frac{zd}{x^2 + z^2} \quad (A62)$$

where $d = \sqrt{x^2 + y^2 + z^2}$

In supersonic flow,

$$u_{SL} = \frac{xd}{\beta^2(x^2 - \beta^2z^2)} \quad (A63)$$

$$v_{SL} = \frac{1}{\beta} \sin^{-1} \frac{\beta y}{\sqrt{x^2 - \beta^2z^2}} \quad (A64)$$

$$w_{SL} = - \frac{zd}{x^2 - \beta^2z^2} \quad (A65)$$

APPENDIX B: DERIVATION OF WING SINGULARITIES

1. Constant Vortex Distribution

The velocity components induced at a point, x, y, z , by a constant vortex distribution on an unswept body panel in supersonic flow are given by equations (A12) through (A14). The velocity components corresponding to a swept, tapered wing panel are obtained by applying a Lorentz transformation about the z -axis. If the leading edge of the panel is swept back through the angle, Λ , and $\lambda = \tan \Lambda$, the three components of velocity may be written:

$$u_{VC} = u'_{VC} - v'_{VC}/\beta^2 \quad (B1)$$

$$v_{VC} = v'_{VC} - \lambda u'_{VC} \quad (B2)$$

$$w_{VC} = \sqrt{\beta^2 - \lambda^2} w'_{VC}/\beta \quad (B3)$$

where u'_{VC} , v'_{VC} , w'_{VC} are given by Eqns. (A12) through (A14), with the following coordinate transformations applied.

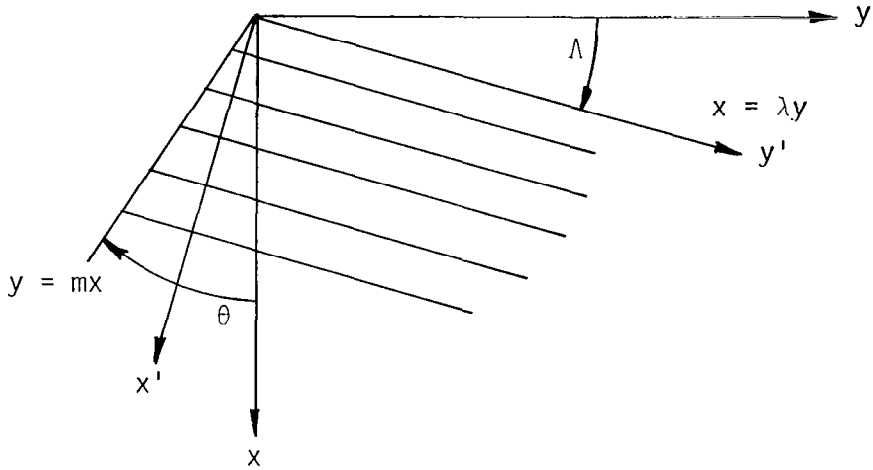
$$x' = \frac{\beta(x - \lambda y)}{\sqrt{\beta^2 - \lambda^2}} \quad (B4)$$

$$\beta y' = \frac{\beta^2 y - \lambda x}{\sqrt{\beta^2 - \lambda^2}} \quad (B5)$$

$$\beta m' = \frac{\beta^2 m - \lambda}{\beta(1 - m\lambda)} \quad (B6)$$

where $m = \tan \theta$.

The geometry is illustrated in the following sketch:



After some simplification, the velocity component formulas for a constant vortex distribution on a panel having arbitrary edge sweep in supersonic flow may be expressed as follows:

$$u_{VC} = F \quad (B7)$$

$$v_{VC} = -\lambda F \quad (B8)$$

$$w_{VC} = (\lambda^2 - \beta^2)H - (\lambda - \beta^2 m)G \quad (B9)$$

where

$$F = \tan^{-1} \frac{(1 - m\lambda) z \sqrt{x^2 - \beta^2(y^2 + z^2)}}{(x - \lambda y)(mx - y) + (\lambda^2 - \beta^2 m)z^2} \quad (B10)$$

$$G = \frac{1}{\sqrt{1 - \beta^2 m^2}} \cosh^{-1} \frac{x - \beta^2 m y}{\beta \sqrt{(y - mx)^2 + (1 - \beta^2 m^2)z^2}} \quad (B11)$$

$$\begin{aligned}
\text{and } H &= \frac{1}{\sqrt{\lambda^2 - \beta^2}} \cosh^{-1} \frac{\lambda x - \beta^2 y}{\beta \sqrt{(x - \lambda y)^2 + (\lambda^2 - \beta^2 z^2)}} && \text{for } \lambda > \beta \\
&= \frac{1}{\sqrt{\beta^2 - \lambda^2}} \cos^{-1} \frac{\lambda x - \beta^2 y}{\beta \sqrt{(x - \lambda y)^2 + (\lambda^2 - \beta^2 z^2)}} && \text{for } \lambda < \beta
\end{aligned}
\tag{B12}$$

It should be noted that, for $m = 0$, Eqns. (B7) through (B9) reduce to Eqns. (108) through (110) of Reference 2.

2. Constant Source Distribution

The velocity components induced at a point, x, y, z , by a constant source distribution on an unswept, tapered body panel in supersonic flow are given by Eqns. (A15) through (A17). The corresponding formulas for a constant source distribution on a wing panel having arbitrary edge sweep in supersonic flow can also be obtained by applying the Lorentz transformation, as described above. The resulting expressions are:

$$u_{SC} = H - mG \tag{B13}$$

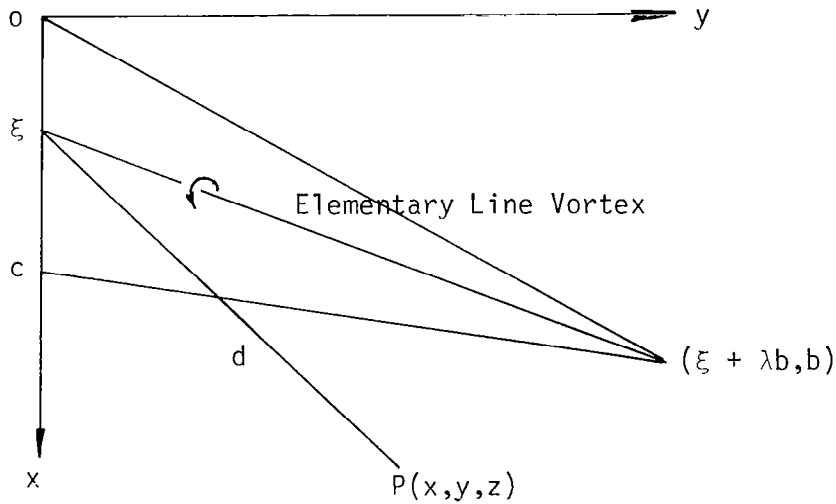
$$v_{SC} = G - \lambda H \tag{B14}$$

$$w_{SC} = -F \tag{B15}$$

where F , G , and H are defined by Eqns. (B10) through (B12). For $m = 0$, the above velocity component formulas reduce to Eqns. (96) through (98) of Reference 2.

3. Constant Edge Vortex Distribution

The constant edge vortex distribution is obtained by combining the influence of a radial vortex distribution on a swept, tapered panel with the constant vortex distribution derived for the same panel. Expressions for the three components of velocity, u_{VC} , v_{VC} , w_{VC} , induced by the constant vortex distribution are given by Eqns. (108) through (110) of Reference 2. Expressions for the velocity components induced by the radial vortex distribution are obtained by integrating the influence of an elementary line vortex of strength, $d\xi$, located along a radial line passing through the intersection of the leading and trailing edges extended. The geometry is illustrated in the following sketch.



In integral form:

$$u_{VR} = z \int_0^c \frac{K}{r^2} d\xi \quad (B16)$$

$$v_{VR} = -\lambda u \quad (B17)$$

$$w_{VR} = - \int_0^c \frac{(x - \xi - \lambda y)K d\xi}{r^2} \quad (B18)$$

where
$$K = \frac{\lambda(x - \xi) + y}{\sqrt{(x - \xi)^2 + y^2 + z^2}}$$

$$r^2 = (x - \xi - \lambda y)^2 + (1 + \lambda^2)z^2$$

and
$$\lambda = \lambda_1 - a\xi/c$$

Here, $a = \lambda_1 - \lambda_2$, $b = c/a$, and λ_1 and λ_2 are the slopes of the leading and trailing edges, respectively. Making the substitution given by Eqn. (51) of Reference 2, and integrating, the velocity components may be written as follows:

$$u_{VR} = \frac{1}{\rho^2} \left\{ (c - ay) F_1 - azG_E \right\} \quad (B19)$$

$$v_{VR} = -\frac{1}{\rho^2} \left\{ (c\lambda - ax) \gamma F_1 \right. \\ \left. + az \left[aD/c - (c - ay)(\beta^2 G_1 + 2(c\lambda - ax)G_E/\rho^2) \right] \right\} \\ + z(x + D)/cr^2 \quad (B20)$$

$$w_{VR} = \frac{1}{\rho^2} \left\{ (c\lambda - ax) \gamma G_E - (c - ay) \left[aD/c - \beta^2(c - ay)G_1 \right. \right. \\ \left. \left. - 2az(c\lambda - ax)F_1/\rho^2 \right] \right\} - y(x + D)/cr^2 \quad (B21)$$

where
$$\gamma = \frac{(c - ay)^2 - a^2z^2}{(c - ay)^2 + a^2z^2}$$

$$D = \sqrt{(x - \xi)^2 + \beta^2 r^2}$$

$$r^2 = y^2 + z^2$$

$$\beta^2 = 1 - M^2$$

$$G_E = (c\lambda - ax)G_1 - G_2$$

and the remainder of the terms are defined by Eqns. (118) through (120) of Reference 2. It should be noted that the influence of a linearly varying line vortex has been added along the side edge of the panel.

The constant edge vortex distribution is obtained by combining the above expressions as follows:

$$u_{VE} = (c_E u_{VR} - u_{VC})/a \quad (B22)$$

$$v_{VE} = (c_E v_{VR} - w_{VC})/a \quad (B23)$$

$$w_{VE} = (c_E w_{VR} - w_{VC})/a \quad (B24)$$

where c_E is the chord length of the edge.

A special case is required for swept constant chord panels ($a = 0$). In this case,

$$u_{VE} = yF_1 - z(\lambda G_1 - G_2) \quad (B25)$$

$$v_{VE} = (x - 2\lambda y)F_1 + z(\beta^2 + 2\lambda^2)G_1 \quad (B26)$$

$$w_{VE} = 2\lambda zF_1 + y((\beta^2 + \lambda^2)G_1 - \lambda G_2) - (x - \lambda y)(\lambda G_1 - G_2) - 2D \quad (B27)$$

4. Constant Vortex Wake

The velocity components induced by a constant vortex wake are obtained by integrating the influence of elementary line vortices located along lines parallel to the x-axis across the panel in a spanwise direction. In incompressible flow,

$$\Delta u_{VW} = 0 \quad (B28)$$

$$\Delta v_{VW} = z \int \frac{d\eta}{(y - \eta)^2 + z^2} \left(1 + \frac{x - \xi - \lambda\eta}{d}\right) \quad (B29)$$

$$\Delta w_{VW} = - \int \frac{(y - \eta)d\eta}{(y - \eta)^2 + z^2} \left(1 + \frac{x - \xi - \lambda\eta}{d}\right) \quad (B30)$$

where $d = \sqrt{(x - \xi - \lambda\eta)^2 + (y - \eta)^2 + z^2}$

Performing the integration,

$$\Delta v_{VW} = F_1 - F_2 \quad (B31)$$

$$\Delta w_{VW} = - \lambda G_1 + G_2 - \log r \quad (B32)$$

where F_1 , F_2 , G_1 and G_2 are defined by Eqns. (99) through (102) of Reference 2.

In supersonic flow,

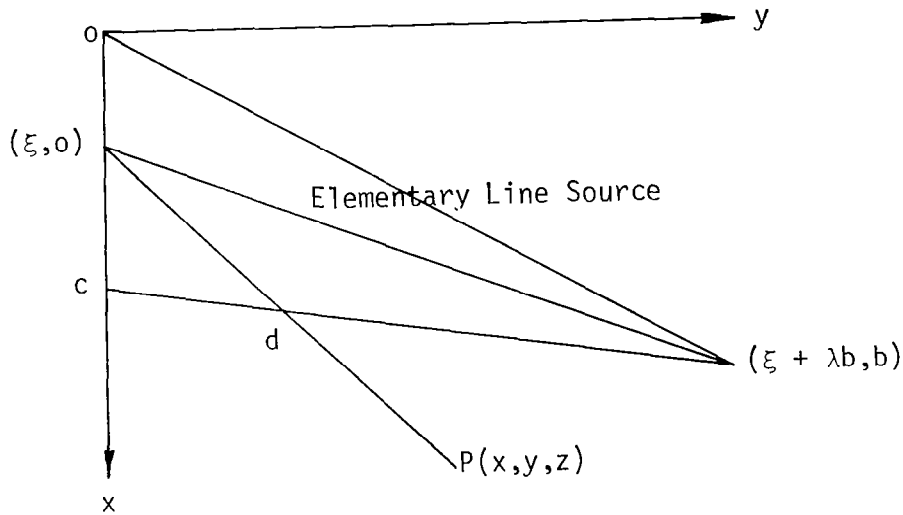
$$\Delta v_{VW} = F_1 \quad (B33)$$

$$\Delta w_{VW} = - \lambda G_1 + G_2 \quad (B34)$$

where G_1 and G_2 are now defined by Eqns. (103) and (104) of Reference 2 .

5. Linearly Varying Source Distribution on a Tapered Panel

The three components of velocity induced at a point, $P(x,y,z)$, by a linearly varying source distribution in the plane of a swept, tapered panel are derived by combining the influences of elementary constant and linearly varying line sources located along radial lines passing through the intersection of the panel leading and trailing edges extended. The geometry is illustrated in the following sketch:



The velocity components are obtained by rotating the line source velocity formulas given in Reference 1 through the angle, Λ , and integrating across the panel chord as follows.

For a constant line source,

$$u_c = \frac{\lambda u_c' - v_c'}{\sqrt{1 + \lambda^2}}$$

$$= \int \frac{(x - \xi - \lambda y)(\lambda(x - \xi) + y)}{(1 + \lambda^2) r^2 d} d\xi - \int \frac{\lambda}{(1 + \lambda^2) d} d\xi \quad (B35)$$

$$\begin{aligned}
v_C &= \frac{\lambda v_C' + u_C'}{\sqrt{1 + \lambda^2}} \\
&= \int \frac{d\xi}{(1 + \lambda^2)d} - \int \frac{\lambda(x - \xi - \lambda y)(\lambda(x - \xi) + y)}{(1 + \lambda^2) r^2 d} d\xi
\end{aligned} \tag{B36}$$

$$w_C = w_C' = z \int \frac{\lambda(x - \xi) + y}{r^2 d} d\xi \tag{B37}$$

where $\lambda = \tan \Lambda = \lambda_1 - a\xi/c$

$$a = \lambda_1 - \lambda_2$$

$$d = \sqrt{(x - \xi)^2 + y^2 + z^2}$$

$$r^2 = (x - \xi - \lambda y)^2 + (1 + \lambda^2)z^2$$

These formulas may be compared with Eqns. (31) through (33) of Reference 2.

For a linearly varying line source,

$$u_L = \frac{\lambda u_L' - v_L'}{\sqrt{1 + \lambda^2}}$$

$$= \int \frac{(x - \xi - \lambda y)d}{(1 + \lambda^2)r^2} d\xi - \int \frac{\lambda}{(1 + \lambda^2)^{3/2}} \sinh^{-1} \frac{\lambda(x - \xi) + y}{r} d\xi \quad (\text{B38})$$

$$v_L = \frac{\lambda v_L' + u_L'}{\sqrt{1 + \lambda^2}}$$

$$= - \int \frac{\lambda(x - \xi - \lambda y)d}{(1 + \lambda^2)r^2} - \int \frac{1}{(1 + \lambda^2)^{3/2}} \sinh^{-1} \frac{\lambda(x - \xi) + y}{r} d\xi \quad (\text{B39})$$

$$w_L = w_L' = z \int \frac{d}{r^2} d\xi \quad (\text{B40})$$

The influences of the constant and linearly varying line sources are multiplied by ξ and combined in the following manner to obtain the final integral forms.

$$u_{SL} = u_C - au_L/c$$

$$= \int \frac{(x - \xi - \lambda y) [(c\lambda_1 - ax)(x - \xi) + y(c - ay) - az^2]}{(1 + \lambda^2)r^2 cd} \xi d\xi$$

$$- \int \frac{\lambda \xi d\xi}{(1 + \lambda^2)d} + \frac{a}{c} \int \frac{\lambda \xi}{(1 + \lambda^2)^{3/2}} \sinh^{-1} \frac{\lambda(x - \xi) + y}{r} d\xi$$

Noting that $\frac{a\lambda\xi}{(1+\lambda^2)^{3/2}} = \frac{1}{\sqrt{1+\lambda^2}} \left(\frac{1+\lambda\lambda_1}{1+\lambda^2} - 1 \right)$, and simplifying,

$$u_{SL} = \frac{1}{c} \int \frac{1}{\sqrt{1+\lambda^2}} \sinh^{-1} \frac{\lambda(x-\xi)+y}{r} d\xi$$

$$- \frac{1}{\sqrt{1+\lambda_2^2}} \sinh^{-1} \frac{\lambda_2(x-c)+y}{\sqrt{(x-c-\lambda_2 y)^2 + (1+\lambda_2^2)z^2}} \quad (B41)$$

The integral appearing in this expressions cannot be evaluated in closed form. It is integrated numerically in the computer program.

$$v_{SL} = v_C - av_L/c$$

$$= \int \frac{\xi d\xi}{(1+\lambda^2)d} + \frac{a}{c} \int \frac{\xi}{(1+\lambda^2)^{3/2}} \sinh^{-1} \frac{\lambda(x-\xi)+y}{r} d\xi$$

$$- \int \frac{\lambda(x-\xi-\lambda y) [(c\lambda_1 - ax)(x-\xi) + y(c-ay) - az^2]}{(1+\lambda^2)r^2 cd} \xi d\xi$$

$$= \frac{1}{a} \left\{ \sqrt{1+\lambda_1^2} \sinh^{-1} \frac{\lambda_1 x + y}{\sqrt{(x-\lambda_1 y)^2 + (1+\lambda_1^2)z^2}} - \lambda_1 G_2 \right.$$

$$- \frac{1}{\rho^2} \left[(c - ay)(e^2 G_1 - (c\lambda_1 - ax)G_2 + aZ(c\lambda_1 - ax)F_1) \right] \} \quad (B42)$$

$$w_{SL} = w_C - aw_L/c$$

$$= \frac{z}{c} \int \frac{\xi}{r^2 d} \left[(c\lambda_1 - ax)(x - \xi) + y(c - ay) - az^2 \right] d\xi$$

$$= \frac{1}{\rho^2} \left\{ sF_1 + z \left[e^2 G_1 - (c\lambda_1 - ax)G_2 \right] \right\} \quad (B43)$$

In incompressible flow, F_1 , G_1 , G_2 , ℓ , s , and ρ are defined by Eqns. (56) through (58) of Reference 2. In supersonic flow, corresponding expressions for these functions are defined by Eqns. (118) through (120).

For $a = 0$, the above velocity component expressions reduce to Eqns. (37) through (39) of Reference 2.

REFERENCES

1. Ehlers., F.E., et al., "A Higher-Order Panel Method for Linearized Supersonic Flow", NASA CR-3062, 1978.
2. Woodward, F.A., "An Improved Method for the Aerodynamic Analysis of Wing-Body-Tail Configurations in Subsonic and Supersonic Flow, Part I: Theory and Application", NASA CR-2228, 1973.
3. Woodward, F.A. and Landrum, E.J., "The Supersonic Triplet--A New Aerodynamic Panel Singularity with Directional Properties", AIAA Journal, Vol. 18, No. 2, February 1980.
4. Woodward, F.A., "USSAERO Computer Program Development, Versions B and C", NASA CR-3227, 1980.
5. Maskew, B. and Woodward, F.A., "Symmetrical Singularity Model for Lifting Potential Flow Analysis", J. Aircraft, Vol. 13, No. 9, September 1976.
6. von Kármán, T. and Moore, N.B., "The Resistance of Slender Bodies Moving with Supersonic Velocities with Special Reference to Projectiles", Transactions of ASME, Vol. 54, 1932, pp. 303-310.
7. Landrum, E.J., "Wind-Tunnel Pressure Data at Mach Numbers From 1.6 to 4.63 for a Series of Bodies of Revolution at Angles of Attack From -4° to 60° ", NASA TM X-3558, 1977.
8. Marconi, F., Salas, M. and Yaeger, L., "Development of a Computer Code for Calculating the Steady Super/Hypersonic Inviscid Flow Around Real Configurations, Volume I: Computational Technique", NASA CR-2675, 1976.
9. Maslen, S.H., "Pressure Distribution on a Thin Conical Body of Elliptic Cross Section at Mach Number 1.89", NACA RM E8K05, 1949.
10. d'Atto, L. Bilyk, M.A. and Sergeant, R.J., "Three-Dimensional Supersonic Flow Field Analysis of the B-1 Airplane by a Finite-Difference Technique and Comparison with Experimental Data", AIAA Paper 74-189, February 1974.
11. Carlson, H.W., "Pressure Distributions at Mach Number 2.05 on a Series of Highly Swept Arrow Wings Employing Various Degrees of Twist and Camber", NASA TN D-1264, 1962.

1. Report No. NASA CR-3466		2. Government Accession No.		3. Recipient's Catalog No.	
4. Title and Subtitle DEVELOPMENT OF THE TRIPLET SINGULARITY FOR THE ANALYSIS OF WINGS AND BODIES IN SUPERSONIC FLOW				5. Report Date September 1981	
				6. Performing Organization Code	
7. Author(s) Frank A. Woodward				8. Performing Organization Report No. AMI Report 8104	
9. Performing Organization Name and Address Analytical Methods, Inc. P.O. Box 3786 Bellevue, WA 98009				10. Work Unit No.	
				11. Contract or Grant No. NAS1-15792	
12. Sponsoring Agency Name and Address National Aeronautics and Space Administration Washington, D.C. 20546				13. Type of Report and Period Covered Contractor Report	
				14. Sponsoring Agency Code	
15. Supplementary Notes Langley Technical Monitor: Emma Jean Landrum Final Report					
16. Abstract A supersonic triplet singularity has been developed which eliminates internal waves generated by panels having supersonic edges. The triplet is a linear combination of source and vortex distributions which gives directional properties to the perturbation flow field surrounding the panel. The theoretical development of the triplet singularity is described together with its application to the calculation of surface pressures on wings and bodies. Examples are presented comparing the results of the new method with other supersonic methods and with experimental data.					
17. Key Words (Suggested by Author(s)) Supersonic Flow Potential Flow Pressure Distribution Panel Method			18. Distribution Statement Unclassified -- Unlimited Subject Category 02		
19. Security Classif. (of this report) Unclassified		20. Security Classif. (of this page) Unclassified		21. No. of Pages 71	22. Price A04